

## Divergence in physical, chemical, and biological soil properties caused by different long-term bare fallow management and natural succession

Steffen Schlüter<sup>a,\*</sup>, Mengqi Wu<sup>a</sup>, Maxime Phalempin<sup>a</sup>, Lena Philipp<sup>b</sup>,  
Evgenia Blagodatskaya<sup>b</sup>, Thomas Reitz<sup>b,c,d</sup>, Carsten Simon<sup>e</sup>, Oliver Lechtenfeld<sup>e</sup>,  
Hans-Jörg Vogel<sup>a</sup>, Martin Schädler<sup>c,f</sup>, Ines Merbach<sup>f</sup>

<sup>a</sup> Helmholtz-Centre for Environmental Research – UFZ, Department of Soil System Science, Halle, Germany

<sup>b</sup> Helmholtz-Centre for Environmental Research – UFZ, Department of Soil Ecology, Halle, Germany

<sup>c</sup> German Centre for Integrative Biodiversity Research (iDiv) Halle-Jena-Leipzig, Leipzig, Germany

<sup>d</sup> Martin Luther University Halle-Wittenberg (MLU), Institute of Agricultural and Nutritional Sciences - Crop Research Unit, Halle, Germany

<sup>e</sup> Helmholtz-Centre for Environmental Research – UFZ, Department of Environmental Analytical Chemistry, Leipzig, Germany

<sup>f</sup> Helmholtz-Centre for Environmental Research – UFZ, Department of Community Ecology, Halle, Germany

### ARTICLE INFO

Handling Editor: Dr Daniel Said-Pullicino

#### Keywords:

X-ray CT

Enzyme activity

High-resolution mass spectrometry

Microbial community composition

Herbicide

Soil tillage

### ABSTRACT

The absence of plants has profound effects on many ecosystem functions of soil. Long-term bare fallow trials are valuable tools for studying the dynamics in soil carbon decline and associated soil degradation. However, it is challenging to disentangle the contribution of missing organic inputs from the frequent physical disturbance caused by soil tillage or herbicide application to keep the soil free from vegetation.

In this study, we evaluate a unique long-term experiment (36 years) in which a bare fallow was established using different methods: i) mechanically through soil tillage, ii) chemically with herbicides, and iii) a combination of both methods. The aim was to separately assess the effects of tillage and herbicide application on various soil properties. Additionally, the bare fallow treatments were compared with natural succession to evaluate the effect of missing organic inputs. We monitored the annual dynamics of carbon and nitrogen contents in the topsoil (0–30 cm) and subsoil (30–60 cm). In addition, we analyzed the shallow topsoil (5–10 cm) comprehensively by integrating physical properties (microstructure and hydraulic properties), chemical properties and biological properties.

All bare fallows were declining in carbon contents at very similar rates while physical disturbance by conventional tillage did not accelerate this effect. In both soil depths of all bare fallows a fast decline in C content during the first ten years was followed by a more gradual or no decline. A large share of the long-term stable carbon was contributed by pyrogenic carbon and to a lesser degree by microbially processed carbon. In the natural succession, the annual increase in soil organic carbon contents was more pronounced in the topsoil than in the subsoil and had not reached a plateau after 36 years.

Irrespective of the bare fallow treatment, the absence of plants ceased the nutrient uplift by roots and the supply of carbon, which drastically reduced all indicators of biological activity like basal respiration, mesofauna abundance, and feeding activity. Soil tillage had a greater impact on the diversity of soil organisms than the application of herbicides. This was due to the disturbance of soil structure, the resulting changes in physical soil properties and the structure of habitats. In addition, tillage effects were stronger for fungal than bacterial communities, as fungal hyphae might be more susceptible to physical disturbance. The bioporosity and especially the amount of empty root channels was elevated in the herbicide fallow to values in the same range as the natural succession, despite the sparse vegetation cover. The fragmentation of the soil matrix by plowing drastically decreased the unsaturated hydraulic conductivity without affecting water retention.

In summary, the frequent physical disturbance by soil tillage had a surprisingly small effect on the quantity and quality of organic carbon, as the decline and shifts in molecular composition were dominated by the absence of organic inputs. In turn, strong effects of physical disturbance were observed for soil properties that depend on pore structure and its persistence in time, like hydraulic conductivity and microbial communities.

\* Corresponding author.

E-mail address: [steffen.schlueter@ufz.de](mailto:steffen.schlueter@ufz.de) (S. Schlüter).

<https://doi.org/10.1016/j.geoderma.2025.117361>

Received 24 March 2025; Received in revised form 16 May 2025; Accepted 21 May 2025

Available online 24 May 2025

0016-7061/© 2025 The Authors. Published by Elsevier B.V. This is an open access article under the CC BY license (<http://creativecommons.org/licenses/by/4.0/>).

## 1. Introduction

Changes in soil carbon stocks result from the balance of organic matter input, redistribution, and mineralization. Land use changes, such as the conversion from croplands to grasslands and vice versa, are known to profoundly affect carbon (C) fluxes (Guo & Gifford, 2002; Post & Kwon, 2000). Whether and how fast a new dynamic equilibrium in C stocks is reached after such a conversion is currently debated, especially concerning the maximum C storage capacity and its soil texture dependency (Poepflau et al., 2024; Six et al., 2024). The C loss in topsoils by conversion of grasslands to tilled cropland is typically much faster, reaching a new dynamic equilibrium within decades, than the slow and steady increase following conversion from cropland to grassland (Or et al., 2021; Poepflau et al., 2011). Our understanding of the underlying mechanisms of these dynamics is limited by the fact that usually the effects of the permanent plant cover and lack of soil cultivation cannot be disentangled, since both factors may have fundamental effects on soil structure, soil biota, and C stocks.

Long-term bare fallows are an extreme variant of such conversions, as carbon inputs cease altogether and C stocks decline at a rate governed by the interplay between various C stabilization mechanisms. Experience from several long-term fallow sites indicates that initial dynamics depend on previous land use while long-term stabilization is mainly related to texture (Barré et al., 2010). Physical protection and stabilization by mineral associations are thought to have a dominant effect on long-term stability, whereas the relative chemical recalcitrance of the compound seems to be more relevant in the short term (Dungait et al., 2012; Lefèvre et al., 2014; Lehmann & Kleber, 2015). A large fraction of this stabilized C is supposed to be derived from microbial biomass (Kallenbach et al., 2016; Liang et al., 2019). Across a range of bare fallow sites, long-term persistent C had a reduced content of energetic C-H bonds, stronger interactions with the mineral matrix (Barré et al., 2016), and higher activation energy, i.e. higher temperature sensitivity of mineralization than more labile organic C (Lefèvre et al., 2014). The chemical signature of this persistent organic C, e.g. in terms of O/C ratios, evolved differently with increasing bare fallow duration across sites which was attributed to different amounts of pyrogenic carbon at each site (Barré et al., 2016). All bare fallow sites had in common that plant-derived compounds decreased in time like lignin, cutin, and suberin, or showed no temporal trend like long-chain alkanes, whereas nitrogen-containing compounds that are usually associated with microbial material were increasing in time (Barré et al., 2018).

Conventional tillage is a common means for soil loosening and litter incorporation. Tillage promotes C mineralization by exposing physically protected C to microbial degradation (Six et al., 1999). This can lead to a strong C loss by infrequent or even individual plowing events in otherwise undisturbed soil (Conant et al., 2007; Peixoto et al., 2020). However, disentangling the role of soil disturbance and missing C input in long-term C stock decline is challenging, as it requires paired long-term no-till and tilled bare fallow trials. Tillage also affects a range of other soil properties. The physical disturbance of soil reduces fungal hyphae length, earthworm abundance, and many other indicators of biological activity (Palm et al., 2014; Verhulst et al., 2010; Young & Ritz, 2000). Tillage destroys continuous biopores but at the same time produces new macropores by fragmentation of the soil so that its net effect of saturated hydraulic conductivity and infiltration capacity is inconsistent, and strongly dependent on site conditions, duration since the last tillage event, and also measurement techniques (Schlüter et al., 2020; Strudley et al., 2008; Wardak et al., 2022). Tillage can also have mixed effects on evaporation depending on the specific operation. Loosening of the soil surface may protect the soil against evaporation losses by inducing capillary barriers, but it can also enhance water losses by increasing surface roughness, providing a larger interface with the atmosphere (Haghighi & Or, 2015; Willis & Bond, 1971).

Likewise, the absence of plants affects not only carbon stocks, but a whole range of physical, chemical, and biological soil properties. A

decline was reported for microbial and mesofauna abundance and activity (George et al., 2021; Hirsch et al., 2009), aggregate stability (Balabane & Plante, 2004; Schweizer et al., 2024), and partly also a degradation of macropore structure (Bacq-Labreuil et al., 2018; George et al., 2021; Neal et al., 2020), each of which may compromise dominant C stabilization mechanisms. In turn, the conversion from bare fallow to annual croplands or perennial grasslands introduces continuous C inputs through plant litter and root exudates, which increases total and labile organic carbon contents, microbial biomass, and mesofauna abundance and thereby can provide degraded soils with the potential for rapid recovery (Hirsch et al., 2017). However, there have been few attempts to reconcile interactions between physical, chemical, and biological soil degradation by measuring several soil properties jointly.

Here, we investigated a long-term experiment (36 years) established in 1988 with mechanical, herbicide and combined bare fallow in combination with a natural succession established on previous cropland to induce carbon depletion and accumulation, respectively. The main objective of the study was to disentangle the effects of the absence of plants and the presence of soil tillage or herbicides on soil degradation. Such a separation is impossible to achieve with other long-term bare fallow trials that do not cover this variety of bare fallow management. We compared the time series of carbon and nitrogen in topsoils (0–30 cm) and subsoils (30–60 cm) to observe the divergence in time. After 36 years, we additionally analyzed the shallow topsoil (5–10 cm) comprehensively by integrating physical properties (bulk density, microstructure, water retention, and unsaturated hydraulic conductivity), chemical properties (pH, nutrients, molecular composition of soil organic carbon) and biological properties (basal respiration, enzyme activity, microbial diversity, and community composition, as well as mesofauna abundance, and feeding activity). We hypothesized that (i) a new C equilibrium would be reached more quickly in bare fallows than in natural succession, as the absence of organic inputs in bare fallows leads to a steady decline in C contents towards some irreducible minimum, whereas continuous plant-derived inputs in natural succession sustain ongoing accumulation. Furthermore, we hypothesized that (ii) the mechanical disturbance by regular plowing would compromise the physical protection of carbon and lead to a faster C mineralization and consequently to a stronger decline of soil organic C in the mechanical and combined bare fallow than in the herbicide fallow. Because of the absence of structure-forming processes like tillage and root growth, we hypothesized that (iii) the herbicide fallow would consolidate by soil settling and therefore feature lower macroporosity and less efficient protection against evaporation. Finally, we expected (iv) a clear impairment of biological activity in the bare fallow compared to natural succession, but the relative importance of tillage compared to herbicides is unclear and should be clarified by this study.

## 2. Materials and methods

### 2.1. Study site and soil sampling

The long-term fallow experiment “V505a” is located at the Experimental Field station of the Helmholtz-Centre for Environmental Research – UFZ, Bad Lauchstädt, and was established in 1988. The site is located in the Central German dry belt (N 51°23', E 11°52', 118 m a.s.l., MAT 9.0 °C, MAP 484 mm) on a Haplic Chernozem soil that was maintained as a cropland before. The trial consists of four treatments: a mechanical bare fallow, a chemical bare fallow, a combined mechanical and chemical bare fallow, and a natural succession. The mechanical fallow and combined fallow are plowed every fall down to 28 cm and plant emergence is reduced with additional rotary cultivator and disc harrow application during the vegetation period. The chemical fallow is kept bare by regular herbicide application (full application history in Table S1) and occasional, careful removal of plants with minimal soil disturbance. The green fallow underwent a natural succession of vegetation, which was only regulated by cutting emerging trees that were left

shredded on the plots. Succession took the typical course for arable fallow land, from annual and biennial weeds (*Chenopodium album*, *Stellaria media*, *Lactuca serriola*) through perennial forbs (*Solidago canadensis*, *Artemisia vulgaris*) to trees (*Sambucus nigra*, *Acer campestre*, *Fraxinus excelsior*) and shrubs (*Rosa canina*, *Cornus sanguinea*, *Rubus caesius*). At the time of sampling, the development was strongly influenced by *Clematis vitalba*. The trial consists of four replicated field plots for each treatment arranged in a regular block design. Each plot has a dimension of 6 x 7 m without buffer strips.

Sampling took place in late April 2024, six months after the last plowing event during a rather moist spring for this region. Topsoil samples were collected at a depth of 5–10 cm. A total of 48 undisturbed soil cores (100 cm<sup>3</sup>, 3 per plot) were acquired to determine bulk density, field water content, basal respiration, and microstructure properties. Larger undisturbed soil cores (250 cm<sup>3</sup>, 1 per plot) were taken from the same depth to determine hydraulic properties. Homogenized soil was collected from the same depth (5–10 cm) around each core for additional chemical and microbiological analysis. Two taller soil cores (280 cm<sup>3</sup> each) were taken at 0–10 cm depth and pooled for mesofauna analysis. The larger volume including the immediate soil surface was required for a sufficiently large number of individuals. Feeding activity was determined in the same depth interval (0–10 cm) as explained below.

In addition, in spring and autumn of every year since 1988, homogenized topsoil and subsoil samples were collected with an auger with an inner diameter of 15 mm from at least twenty different locations per plot at a depth of 0–30 cm and 30–60 cm, respectively.

## 2.2. Physical and microstructure measurements

Bulk density and volumetric field water contents were determined after oven-drying intact soil cores for 48 h at 105 °C. Soil water retention curves and unsaturated hydraulic conductivity were measured with the evaporation method (Hyprop, METER Group) down to matric potentials of > -10000 hPa (< pF 4). Additional water retention information at very negative matric potentials of < -10000 hPa was determined with the dew point hygrometer method (WP4C, METER Group).

Microstructure analysis of intact soil cores was done with an X-ray computed microtomograph (X-Tek XT H 225, Nikon Metrology) prior to oven-drying of the samples. Beam properties were set to 130 kV and 150 µA using a 0.1 mm copper filter for reducing beam hardening artifacts. 2500 projections with one frame per projection were acquired with an exposure time of 708 ms per frame. Tomograms were reconstructed in 8-bit grayscale and with a voxel size of 30 µm using the X-tek CT Pro software (Nikon Metrology). Grayscale contrast was stretched by setting the darkest and brightest 0.2 percentiles to 0 and 255, respectively.

The raw image were cut into the largest possible cylindrical regions of interest without visible soil disturbances. Vertical and radial differences in average gray values were corrected (Schlüter et al., 2016). All gray-scale images were segmented using nnU-Net, a self-configuring method for deep learning-based image segmentation (Isensee et al., 2021). Based on the visual analysis of the images, eight material classes were identified. For the mineral phase, we differentiated the soil matrix and denser particles such as sand grains or concretions. For the pore phase, we identified three classes, i.e., the (i) cracks and irregular pores created by abiotic factors such as tillage, wetting–drying, or freeze–thaw cycles and the biopores created by biotic factors such as root growth or bioturbation. The biopore class was further subdivided into two classes: the (ii) root-induced empty channels left after the decay of roots and the (iii) earthworm burrows created after the passage of earthworms and ground-nesting bees. For the organic phase, we distinguished “living roots and the “root residues”, which were root-like objects with a lower gray value than the living roots. We also identified the “other POM” class which was considered to be POM that was not root-derived (e.g., seeds, straw pieces, litter, or leaf fragments).

Note that this new deep-learning-based segmentation method

enabled to segment an unprecedented number of material classes, while effectively reducing the amount of false positives and increasing segmentation accuracy (Phalempin et al., 2025). The classifier was trained with manual annotations for the aforementioned material classes drawn independently by two experts on twenty selected sub-volumes, which were distributed equally among cropland and grassland samples in an adjacent long-term trial. Training and segmentation with nnU-Net were carried out on a high-performance computing cluster equipped with eight GPU nodes, each of them hosting NVIDIA A100 80G GPU accelerators (GPGPU), which could be requested via a job scheduling system. For more information regarding the segmentation procedure, the reader is referred to (Phalempin et al., 2025).

The microstructure of segmented images was analyzed with respect to volume fractions of different classes using Fiji/ImageJ (Schindelin et al., 2012). Pore structure was analyzed by combining fresh root, root residues, other POM, empty root channel, earthworm burrow, and other abiotic pores into a composite class as this corresponds to the visible pore space after all POM was mineralized. The average pore diameter was calculated with the local thickness method in Fiji/ImageJ. In addition, the bioporosity was analyzed by excluding the abiotic pore class that does not have a cylindrical shape.

## 2.3. Chemical measurements

Total organic carbon (TOC), total nitrogen (TN), and mineral nitrogen (nitrate + ammonium) have been continuously measured since 1988 in homogenized soil samples taken from the topsoil (0–30 cm) and subsoil (30–60 cm) in autumn, with additional measurements of mineral nitrogen in spring. The analysis was carried out for TOC and TN with elemental analysis after dry combustion (DIN ISO 13878, 1998) and for NO<sub>3</sub>-N and NH<sub>4</sub><sup>+</sup>-N photometrically with the N<sub>min</sub> laboratory method (VDLUFA I, A 6.1.4.1 method in Verband Deutscher Landwirtschaftlicher Untersuchungs-und Forschungsanstalten (VDLUFA) (2007)).

Water-extractable organic carbon (WEOC) and water-extractable total nitrogen (WETN) were extracted from 5 g of shallow topsoil (5–10 cm depth) with 0.05 M K<sub>2</sub>SO<sub>4</sub> in a 1:4 ratio and determined by a C/N analyzer (Multi N/C 2100 analyzer, Analytik Jena). Available phosphate and potassium in the soil were extracted with double lactate solution (1:50 w/v) at pH 3.6. Phosphate contents were determined colorimetrically using the molybdenum blue method (Murphy & Riley, 1962), while potassium was measured from the same extract using an ion-selective electrode (perfectION comb K, Mettler-Toledo). For pH measurements, 12 g of air-dried soil was suspended in 30 ml of 0.01 M CaCl<sub>2</sub>, shaken for 1 h, and measured with a pH electrode (SevenEasy pH meter, Mettler Toledo).

To assess the molecular composition of soil organic C, milled soil samples were measured by laser desorption/ionization Fourier transform ion cyclotron resonance mass spectrometry (LDI-FT-ICR-MS) (Simon et al., 2025; Solihat et al., 2019). Mixing 50 µg of sample with 150 µl of ultrapure water (MilliQ Integral 5, Merck) in an acid-washed micro test tube (Th. Geyer) yielded a suspension with 25 ± 2 % soil dry weight. The mixture was shaken thoroughly, vortexed for 15 s, and 5 µl of the suspension was immediately spotted onto a ground steel target (MTP 384 target plate ground steel BC, Bruker Daltonics) and left to air-dry under a fume hood. Each sample was spotted three times to allow replicate measurements. Here, we used a dual source ESI/MALDI-FT-ICR mass spectrometer equipped with a dynamically harmonized analyzer cell (solariX XR, Bruker Daltonics) and a 12 T cooled actively shielded superconducting magnet (Bruker Biospin). We used Compass DataAnalysis 5.0 (Bruker Daltonics) for processing raw mass spectra. Mass spectra were exported after peak selection at a signal-to-noise ratio of 4. The mass lists were then exported and further processed with in-house software (Wurz et al., 2024). Molecular formulas were assigned based on the following rules: even electron configuration, mass range: 0–1,000 Da, mass error tolerance: ±0.5 ppm, O/C ratio: 0–1.2, H/C

ratio: 0–3, N/C ratio: 0–1.5, double bond equivalents (DBE): 0–50; DBE-O: –10–30; element ranges of major isotopes: 12C: 1–80, 13C: 0–1, 1H: 1–198, 14N: 0–5, 16O: 0–40, 32S: 0–3, 34S: 0–1). After the removal of formulas with multiple assignments, formulas occurring only once across all samples, and formulas occurring only once across triplicates, the final dataset contained 13,501 unique formulas. Further details on FT-ICR-MS measurements and data processing are given in the Supplementary Information (Note S1). Based on the stoichiometry of the formulas, we calculated intensity-weighted averages (i.e., intense peaks contributed more to the average) of the following properties as aggregated properties of each mass spectrum: H/C ratio (“H/C”), O/C ratio (“O/C”), molecular weight (“MW”), double bond equivalents (“DBE”), modified aromaticity index (“AI<sub>mod</sub>”), (Koch & Dittmar, 2006, 2016), nominal oxidation state of C (“NOSC”, (Riedel et al., 2013)), Gibbs energy of half oxidation ( $\Delta G_{\text{Cox}}^0$ , (LaRowe & Van Cappellen, 2011)), and formula classes (containing only oxygen besides C and H, “CHO”; containing additional N or S, “CHNO” or “CHOS” respectively; containing O, N, and S, “CHNOS”; and the remaining classes CH, CHN, CHS, and CHNS accordingly if no O contained). Predefined molecular groups were considered following Hawkes et al. (2020): Condensed aromatics (“CA”); aromatics (“AR”); highly saturated highly oxidized (“HO”); highly saturated less oxidized (“LO”); and aliphatics (“AL”). Absolute and relative numbers and relative intensity share were calculated for each formula class and compound group.

#### 2.4. Biological measurements

Basal respiration of intact soil cores was measured at 22 °C using an automated respiration analyzer (Respicond V, Respicond) prior to X-ray CT scanning. During the measurements, the respired CO<sub>2</sub> was trapped by an alkali solution (10 mL of 0.6 M KOH solution) placed in the headspace of the sample container. Changes in the electrical impedance of the alkali solution were then used to calculate CO<sub>2</sub> concentration. Incubations were carried out 1–2 days after sampling and lasted more than one day. The final hours were considered for averaging during which the respiration rates were stable.

Extracellular soil enzyme activities were measured using a fluorometric assay (Sinsabaugh et al., 2003). The activity potentials of three hydrolytic soil enzymes ( $\beta$ -glucosidase, N-acetylglucosaminidase, and phosphatase), which are involved in the microbial acquisition of carbon, nitrogen and phosphorous, were quantified in MES buffer at pH 6.15 via 4-methylumbelliferon (MUF)-coupled substrates. In addition, the activity of Leucin-aminopeptidase, which is also involved in the microbial acquisition of N, was determined at pH 8 (TRIZMA buffer) using L-Leucin-7-amido-4-methylcumarinhydrochlorid. Soil suspensions were incubated with the four different substrates in 96-well microplates at room temperature for 1 h. Fluorescence that was induced by cleavage of the substrate and the consequent release of the fluorophores (MUF and AMC) was measured at 360 nm excitation and 460 nm emission wavelengths.

For microbial community analysis, DNA was extracted from soil using the Qiagen DNeasy PowerSoil Pro Kit following the manufacturer’s protocol. Bacterial target 16S-rDNA-fragment and fungal target ITS2-region were amplified in a PCR using primers (515f: GTGY-CAGCMGCCGCGGTAA, 805r: GGACTACHVGGGTWTCTAAT for 16S rDNA and ITS4: TCCTCCGCTTATTGATATGC and fITS7: GTGART-CATCGAATCTTTG for ITS2 region) and the KAPA HiFi DNA polymerase. PCRs were conducted in triplicates for each sample and pooled afterwards. PCR products were purified with AmpPure XP Beads and indexed with Illumina Nextera XT index primers in another PCR. PCR products were purified again with AmpPure XP Beads and DNA concentration was determined using a Nanodrop ND-8000 Spectrophotometer. Samples were equimolarly pooled to a bacterial and a fungal pool, respectively. Final pool concentrations were determined with Qubit. Bacterial and fungal pools were prepared for paired-end sequencing with the MiSeq Illumina v2 reagent kit according to manufacturer’s instructions and

injected into an Illumina MiSeq flow-cell. Sequencing reads were processed in the dada2 pipeline (version 11) (Weißbecker et al., 2020) including primer removal, quality filtering, chimera removal and ASV with mothur classifier and taxonomic assignment using the SILVA 138 SSU database for 16S rDNA and UNITEv10 for ITS2 region. Microbial biomass carbon ( $\mu\text{g g}^{-1}$ ) was estimated from DNA concentrations ( $\mu\text{g g}^{-1}$ ) with a conversion factor of 5.6 (Joergensen et al., 2024).

In-situ soil invertebrate decomposer activity was assessed by applying the bait lamina test (Kratz, 1998). In brief, we used PVC strips with 16 perforations with 1.5 mm diameter arranged in 5 mm distance. The bait holes were filled with a mixture of cellulose powder (70 %), wheat bran (27 %) and activated charcoal (3 %). Four strips per plot were inserted vertically into the soil at randomly chosen locations with the uppermost hole just beneath the soil surface. After two weeks of exposure, the strips were removed from the soil and each hole was inspected and the bait was rated as either 0 % (no feeding activity), 50 %, or 100 % consumed (high feeding activity). Mean bait consumption per strip was calculated before statistical analyses.

Soil fauna was sampled with two soil cores (6 cm diameter, 10 cm depth) per plot taken within a radius of 20 cm to the bait lamina strips and extracted in a MacFadyen high-gradient extractor for 10 days (Macfadyen, 1961). The abundance of the extracted fauna was assessed under a microscope after determination to order level.

#### 2.5. Statistical analysis

Statistical analysis was done in R version 4.2.2 (R Core Team, 2022). Statistical analysis of most chemical, physical, and biological properties followed the same protocol. The normality of residuals was assessed visually and data were log-transformed if necessary. Homogeneity of variances was assessed with Levene’s test implemented in the car package (Fox & Weisberg, 2011). Linear mixed-effects models with random block intercepts were implemented to evaluate treatment effects on various soil properties using the lme4 package (Bates et al., 2015). Pair-wise differences between estimated marginal means were tested for significance at  $p < 0.05$  after Bonferroni adjustment for multiple comparisons using the emmeans package (Lenth, 2022). The Games-Howell test in the user friendly science package (Peters & Gruijters, 2023) was used for heteroscedastic data. All plots were generated with the ggplot2 package (Wickham, 2016).

The statistical analysis of the molecular composition of organic matter followed a different protocol. To assess the similarity in molecular composition, all mass spectra were normalized to an arbitrary summed intensity of 1, Bray-Curtis dissimilarity was computed, and the dissimilarity matrix was used to perform Principal Coordinates Analysis (PCoA). Linear gradients of aggregated mass spectrum indices were plotted onto the ordination to identify general trends in organic matter compositional variation across samples. Formulas significantly correlated with both principal coordinates ( $p < 0.05$ ) in were visualized in Van Krevelen space, according to their unique O/C and H/C ratios (Kim et al., 2003). Based on the separation of samples in the PCoA we aimed to identify the formulas that differentiated a) “Succession” from “Combined” treatment and b) “Mechanical” from “Herbicide” treatment. We isolated those formulas that either only occurred in one of the two treatments or had a significantly higher ion abundance in one treatment compared to the other.

Microbial community was analyzed using the phyloseq (McMurdie & Holmes, 2013) and vegan packages (Oksanen et al., 2025). Sequences assigned to chloroplasts and mitochondria were removed prior to analysis. Data were normalized with DESeq2. Alpha diversity indices were calculated with the “estimate\_richness” function in phyloseq. Statistical significance was determined using a linear-mixed effects model in the lme4 package (Bates et al., 2015) with treatment as fixed effect and Block as random effect. Beta-diversity was determined with Bray-Curtis dissimilarity and principal coordinate analysis (PCoA) using a 10 % prevalence filtered data set. Statistical significance of Bray-Curtis

dissimilarity was calculated with PERMANOVA (adonis2 function) with a model including treatment as the fixed effect, Block as random effect and 999 permutations. To analyze within group differences of the four treatment types, pairwise PERMANOVA was conducted using the pairwise.adonis function.

### 3. Results

#### 3.1. Long-term dynamics

The topsoil carbon contents initially amounted to approximately  $20 \text{ mg g}^{-1}$  and declined monotonously by 20 % towards  $16 \text{ mg g}^{-1}$  in all three bare fallows with a faster decline during the first ten years (Fig. 1a). The arithmetic mean of the last four years did not differ between bare fallow treatments ( $p > 0.05$ , Fig. S1b). In contrast, natural succession steadily accumulated carbon with some acceleration after the first years without reaching a plateau after 36 years. The comparison of carbon contents in 5–10 cm (measured in 2024) and 0–30 cm (average of 2021–2024) indicates a stratification in the topsoil under natural succession that is absent under all bare fallows (Fig. S1a-b). Initial carbon contents in the subsoil amounted to  $16\text{--}17 \text{ mg g}^{-1}$  and also declined by 20 % to  $13\text{--}14 \text{ mg g}^{-1}$  during the first 10–15 years under bare fallow after which the values remained constant (Fig. 1e). The mechanical bare fallow treatments reached lower carbon contents than the herbicide bare fallow ( $p = 0.046$ , average of 2021–2024) with the combined bare fallow ranging in between (Fig. S1c). In the natural succession, there was no build-up of carbon contents in the subsoil.

Topsoil nitrogen contents showed similar temporal evolution compared to organic carbon contents (Fig. 1b) with C:N ratios fluctuating around a constant value of 11.6 (Fig. 1c). An accelerated TN loss in the topsoil of bare fallows after 30 years caused a gradual increase in C:N ratios to 13, which did not occur in the natural succession. In the subsoil, TN remained constant in the natural succession, whereas bare fallows lost TN at a constant rate. In combination with the non-linear dynamics of TOC contents, this caused a decrease in C:N ratios during the first

10–15 years, followed by an increase in all treatments.

Mineral nitrogen contents in the topsoil (Fig. 1d) and subsoil (Fig. 1h) exhibited the highest discrepancy between treatments in the first five years of the long-term experiment, when the decomposition of plant residues released mineral nitrogen in the bare fallows, whereas a net loss occurred during the build-up of plant biomass in the natural succession. Afterwards, a steady decline in  $N_{\text{min}}$  contents occurred in the topsoil of bare fallows, whereas the recycling of standing biomass in natural succession evoked a 4-fold (spring) and 1.7-fold increase (autumn) in  $N_{\text{min}}$  contents compared to bare fallows.  $N_{\text{min}}$  contents in the subsoil were very similar after five years among all treatments. Relative contributions of ammonium and nitrate fluctuated strongly during the first twenty years of the experiment and then converged to a dominance of nitrate in all treatments and depths (Fig. S2).

#### 3.2. Chemical properties of the topsoil

Water-extractable organic carbon (Fig. 2a) and water-extractable total nitrogen (Fig. 2b) in topsoils were three times lower in bare fallows compared to the natural succession. Also when normalized by TOC, carbon tended to be less soluble under bare fallows ( $p = [0.01\text{--}0.16]$ , Fig. S3). The available potassium content (Fig. 2c) was approximately six times higher in the natural succession than in the bare fallows. In contrast, available phosphorous did not differ between natural succession and bare fallows. The pH value was slightly reduced in the herbicide bare fallow (Fig. 2d), but the difference did not exceed spatial variation ( $p = 0.16$ ).

The LDI-FT-ICR-MS data revealed a clear clustering of succession vs. bare fallows along the first coordinate (Fig. 3), representing the largest share of variability in molecular composition (62 %). Bare fallows were separated from one another on coordinate 2, representing the next largest share of variability present in the dataset (9 %). Notably, we observed a difference between the mechanical and herbicide fallow along coordinate 2, with the combined treatment falling in between (Fig. 3). Formulas associated with the bare fallow samples were

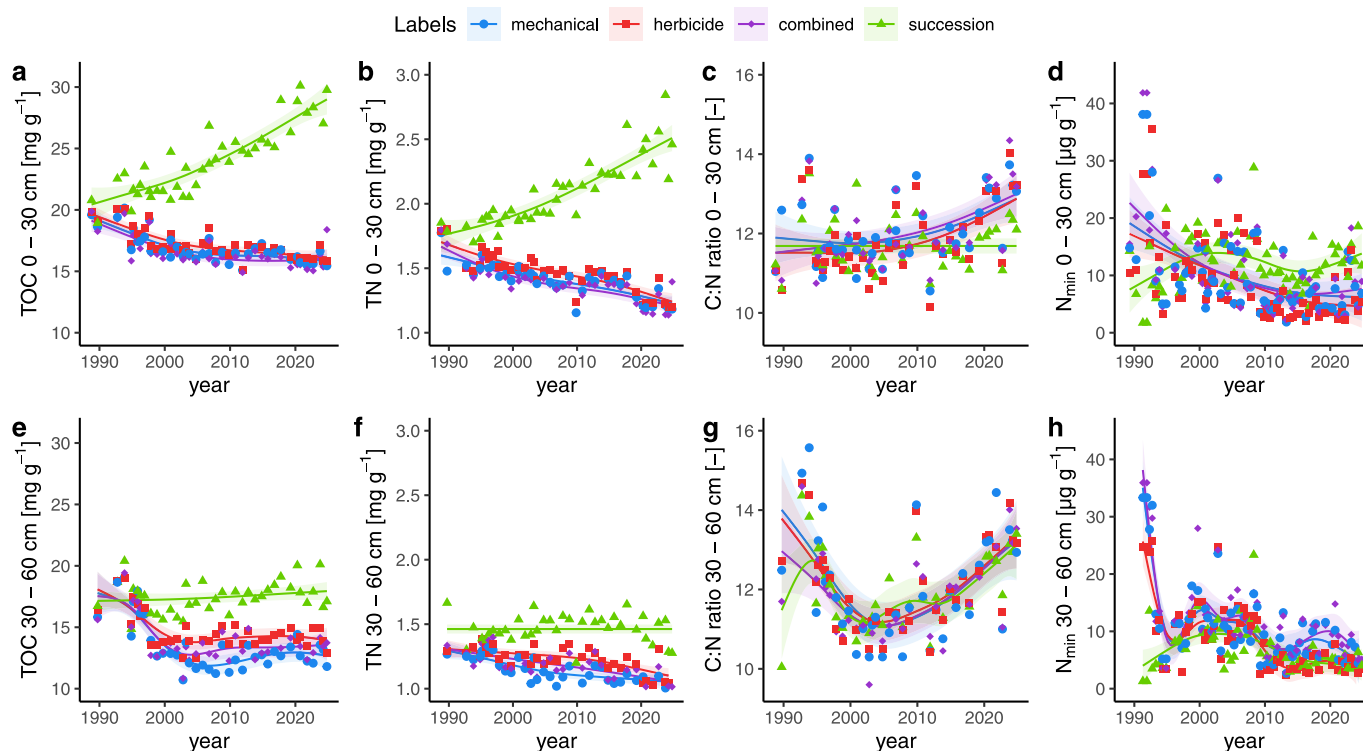


**Fig. 1.** Time series of average total organic carbon, total nitrogen, C:N ratio, and mineral nitrogen in the topsoil (a-d) and subsoil (e-h). Trendlines represent generalized additive models with confidence intervals.

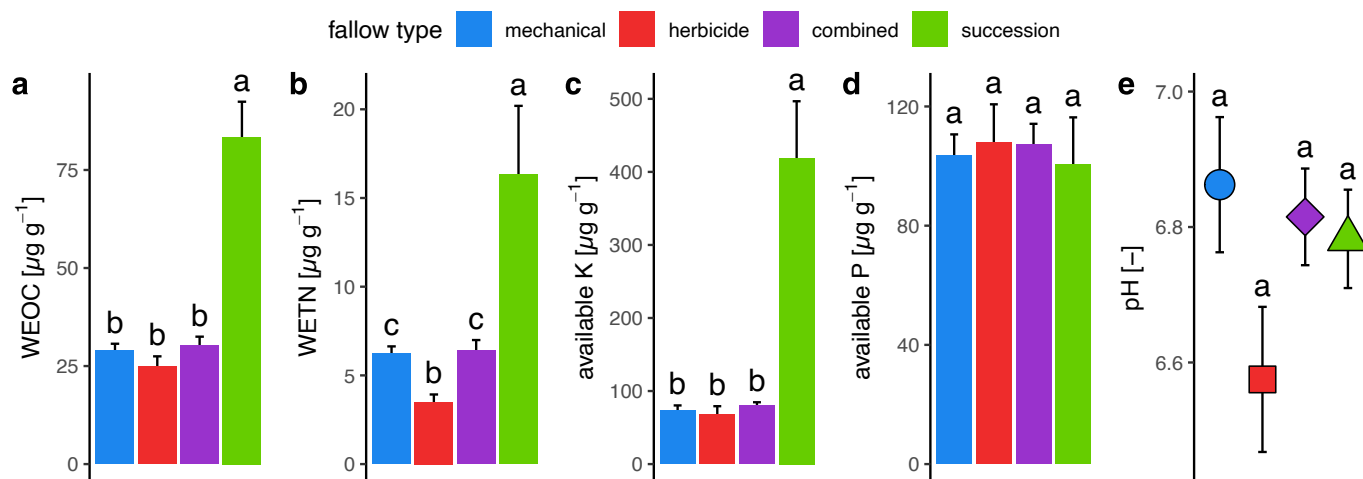


Fig. 2. Chemical properties (mean  $\pm$  standard error,  $n = 4$ ) of all fallow treatments (WEOC – water extractable organic carbon, WETN – water extractable total nitrogen). Different letters indicate significant differences between treatment means tested at  $p = 0.05$ .

dominated by condensed aromatic and aromatic compounds and some compounds indicative of microbial biomass (aliphatics), whereas succession-associated formulas were dominated by less condensed, saturated, and oxidized compounds, and can be interpreted as plant-derived by experimental design (Correlation with Coordinate 1, Fig. S4a). A subsequent analysis of the formulas discerning succession from bare fallow samples revealed a lower molecular weight, lower numbers of C but higher numbers of H and O atoms per formula, enrichment in all elemental ratios (H/C, O/C, N/C, and S/C), and lower aromaticity in succession samples (Table S2). The relative share of condensed aromatic compounds and CH, CHN and CHOS formulas was higher in bare fallow samples (represented by combined bare fallow in Fig. S4a and Fig. 3). In contrast, formulas explaining the difference between mechanical and herbicide fallow were less numerous (Correlation

with Coordinate 2, Fig. S4b). A subsequent analysis of the formulas discerning these fallow types revealed a higher molecular weight, lower aromaticity, lower oxidation state, and lower numbers of all elements except S in herbicide fallow samples (Table S3). The relative share of CHNO and CHN formulas, and condensed aromatics was higher in the mechanical fallow, while the herbicide fallow showed higher shares of CHO and CHOS formulas (Fig. S5c, d). CHN and CHOS formulas showed a high specificity towards mechanical and herbicide fallows, respectively (Fig. S5c, S4d, e).

The activity of hydrolytic enzymes (Fig. 4) was elevated under natural succession but did not differ between bare fallows ( $p > 0.05$ ). The differences between natural succession and bare fallows varied among the specific enzymes. It was 3.4-fold, 6.8-fold, 12.4-fold, and 13-fold elevated for phosphatase, Leucin-aminopeptidase, beta-glucosidase and N-acetyl-glucosaminidase, respectively.

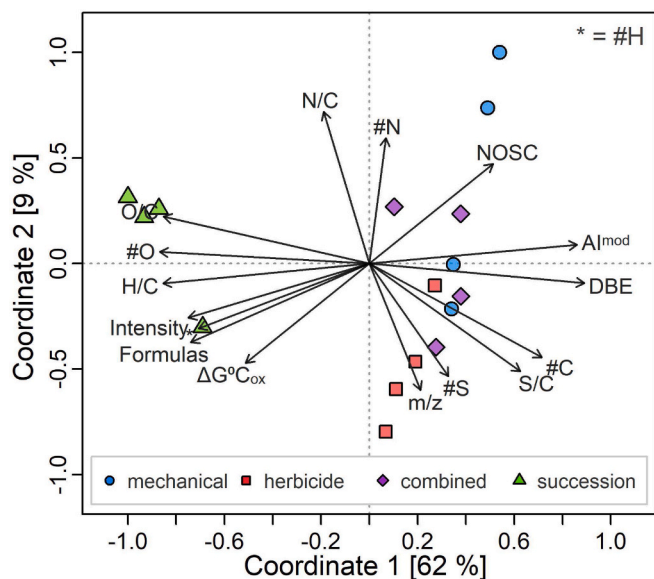


Fig. 3. Principal Coordinate Analysis of compositional trends derived from LDI-FT-ICR-MS measurements of soil samples. Coordinate labels indicate percent explained variation. The ordination was based on ion abundances of all molecular formulas ( $n = 13501$ ). Arrows represent significant linear correlations of aggregated chemical indices of each mass spectrum (see section 2.3) with both coordinates. Arrow direction indicates correlation tendency (with coordinate 1, 2, or both) and arrow length indicates strength of correlation. Label of chemical parameter #H (intensity-weighted average number of H atoms per formula) replaced by an asterisk to omit over-plotting.

### 3.3. Biological properties

All indicators of biological activity were reduced in the bare fallows compared to natural succession. Basal respiration (Fig. 5a) and mesofauna feeding activity (Fig. 5c) were 3.1-fold and 2.4-fold increased, respectively. Microbial biomass carbon was 7.9-fold elevated in the natural succession (Fig. 5b). When normalized by TOC, microbial biomass was still elevated under natural succession, but basal respiration was not. There was a trend towards higher mesofauna abundances in the natural succession ( $p = 0.13$ ) compared to the combined fallow with rather high variability among replicates in all treatments (Fig. 5c). The bare fallows did not differ from each other in any of the biological properties, except for lower microbial biomass carbon in the combined fallow as compared to the herbicide fallow.

The richness and diversity of soil microbial communities varied among different fallow types (Fig. 6, Fig. S7). Observed fungal richness was highest in the natural succession and lowest in the herbicide fallow. The Shannon index of fungi followed a similar pattern, with the natural succession supporting greater diversity than the bare fallows (Fig. 6b). In contrast, bacterial richness was not different across fallow types. However, mechanical and combined bare fallows exhibited slightly higher values than the herbicide bare fallow and natural succession. The same pattern emerged for the Shannon index of bacteria, with lowest diversity in the herbicide bare fallow.

The composition of bacterial phyla was relatively consistent across treatments, with nine phyla representing 95–96 % of bacterial taxa (Fig. 7a and Table S6). Actinobacteria (28–33 %) and Acidobacteria (10–13 %) were among the most dominant phyla. Both showed little response to the fallow type. Proteobacteria also represented a large

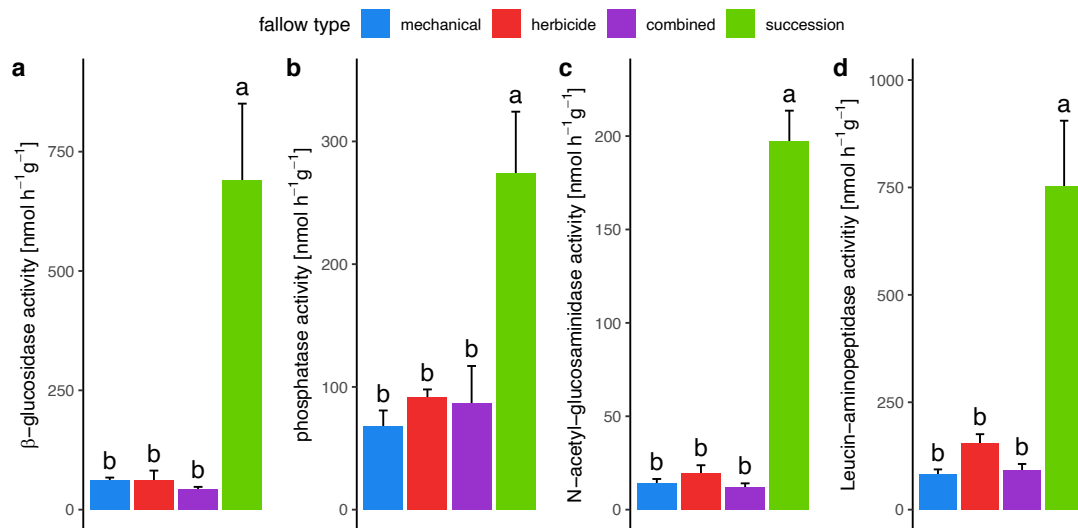


Fig. 4. Activity of hydrolytic enzymes indicative of carbon, phosphorus, and nitrogen cycling (mean  $\pm$  standard error,  $n = 4$ ). Significant differences in treatment means were tested at  $p = 0.05$ .

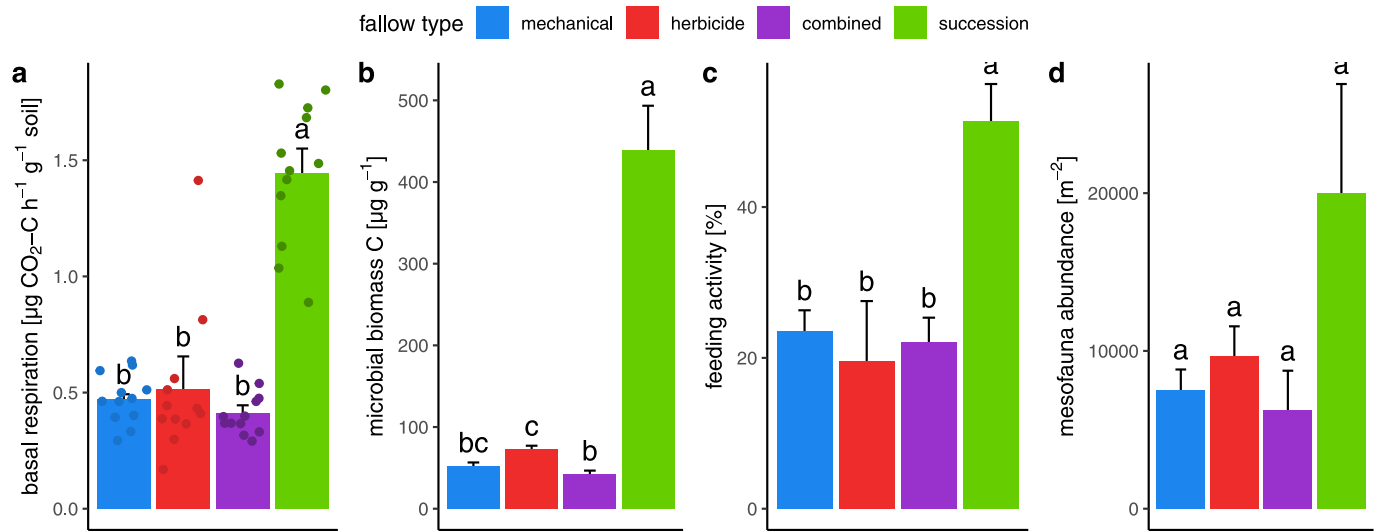


Fig. 5. Indicators of microbial (a-b) and mesofauna (c-d) activity (mean  $\pm$  standard error,  $n = 4$ ). Jitter points in (a) correspond to individual soil cores ( $n = 16$ ). Significant differences in treatment means were tested at  $p = 0.05$ .

proportion of the bacterial community, but their relative abundance was increased in the natural succession (23 %), while decreased in the herbicide bare fallow (13 %), with the two other bare fallows in between (17 %). In contrast, Firmicutes were strongly decreased in the natural succession (3 %) compared to all bare fallows (11–13 %). The relative abundances of the remaining phyla ranged between 1 % and 8 % and did not show significant responses to the fallow type.

The fungal phyla composition showed more pronounced differences (Fig. 7b, Table S6). Ascomycota dominated across all fallow types, but their relative abundance varied strongly, with 69 % in the succession fallow, 55 % in the herbicide fallow, but only 47 % in the two plowed fallows (mechanical and combined). In the same manner, the relative abundance of Basidiomycota in the plowed fallows was only half of the abundance in the other two fallows. In contrast, Chytridiomycota and Mortierellomycota showed a significantly higher relative abundance in the two plowed fallows compared to the herbicide bare fallow and natural succession.

Principal Coordinates Analysis revealed a clear separation of bacterial (Fig. 8a) and fungal (Fig. 8b) communities according to fallow type.

For bacteria and fungi, the first two principal coordinates explained a substantial proportion of variance (bacterial communities: PCoA1: 49.5 %, PCoA2: 20.3 %; fungal communities: PCoA1: 31.7 %, PCoA2: 18.1 %). For both organism groups, the soil communities in the succession and herbicide fallows formed distinct clusters, while those of the mechanical and combined fallows were positioned close together, indicating high similarity. PERMANOVA analysis confirmed that bacterial and fungal communities differed between all fallow types except for mechanical and combined fallows (Table S5).

### 3.4. Structural properties

Representative 2D grayscale sections and 5 mm thick 3D sub-volumes of pores (gray) and POM (red) around these 2D sections revealed vast differences in soil microstructure (Fig. 9). The mechanical and combined fallow featured the typical morphology of a tilled soil with a fairly loose packing of differently sized fragments produced by tillage. The pore morphology of the herbicide treatment was more similar to that of a natural succession with a dense network of refilled or

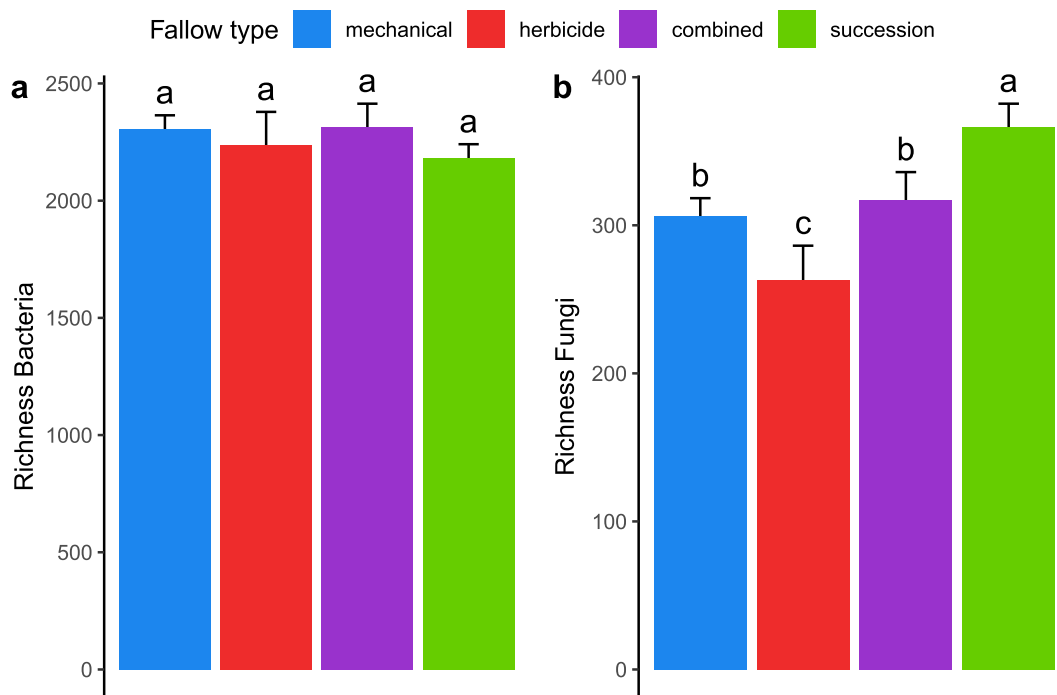


**Fig. 6.** Richness of bacterial and fungal communities (mean ± standard error,  $n = 4$ ) in different fallow types. Statistically significant differences are indicated with letters, p-values are summarized in Table S3.

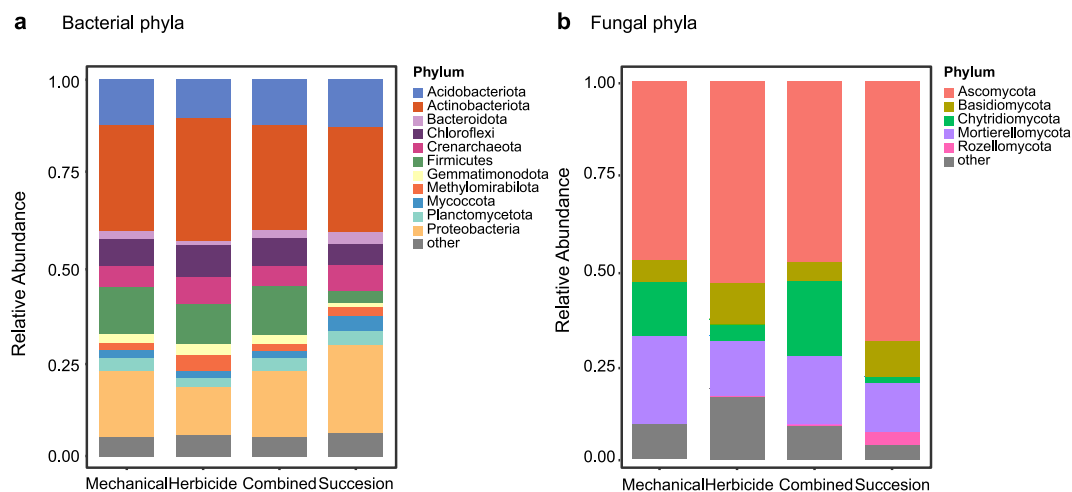


**Fig. 7.** Relative abundance of dominant (a) bacterial and (b) fungal phyla in different fallow types. Other and unassigned phyla are grouped as other. Relative abundance values are summarized in Table S5.

empty biopores. The natural succession featured a network of curvy cracks along old biopores and casts that was also visible, but less distinct in the herbicide treatment. The natural succession was rich in POM, mostly as elongated root residues. POM in the bare fallows was less abundant and mainly in the form of small particles with a rounded shape, which is a typical morphology of pyrogenic carbon abundant in the soils of the study region. The separation of POM into living roots, root residues, and other POM for all samples (Fig. S8) indicated that (i) living roots were very abundant in all soil cores from natural succession, but only present in a few of the soil cores from bare fallows, (ii) that herbicide bare fallow harbored more root residues than other bare fallows, and (iii) that other POM was present in all soil cores with considerable variability among soil cores from the same treatment.

These visual differences between fallows were confirmed by structure analysis. Bulk density increased in the order succession (1.26 g/

$\text{cm}^3$ ) < herbicide fallow (1.41 g/ $\text{cm}^3$ ) < mechanical fallow (1.52 g/ $\text{cm}^3$ ) <= combined fallow (1.56 g/ $\text{cm}^3$ ) (Fig. 10a). Both tilled fallows featured the greatest variability at the core level (jitter points in Fig. 10a) with some samples in the range of the herbicide fallow and some very compact samples, indicating a random chance to hit rather loose areas during sampling or dense clods larger than the sampling ring itself. The bulk density of the bare fallows increased with decreasing TOC content ( $R = -0.65$ , Fig. S9). Visible porosity comprises macropores larger than 60  $\mu\text{m}$  which can be detected at a voxel size of 30  $\mu\text{m}$ . This macroporosity features even greater variability at the core level in the tilled soils (Fig. 10b). This spatial variability, which is mainly contributed by macropores of non-biological origin, persists at the plot level (error bars in Fig. 10b) and renders the 35 % drop in tilled soils insignificant. Bioporosity was destroyed by plowing and was two times higher in the natural succession compared to the herbicide fallow. When

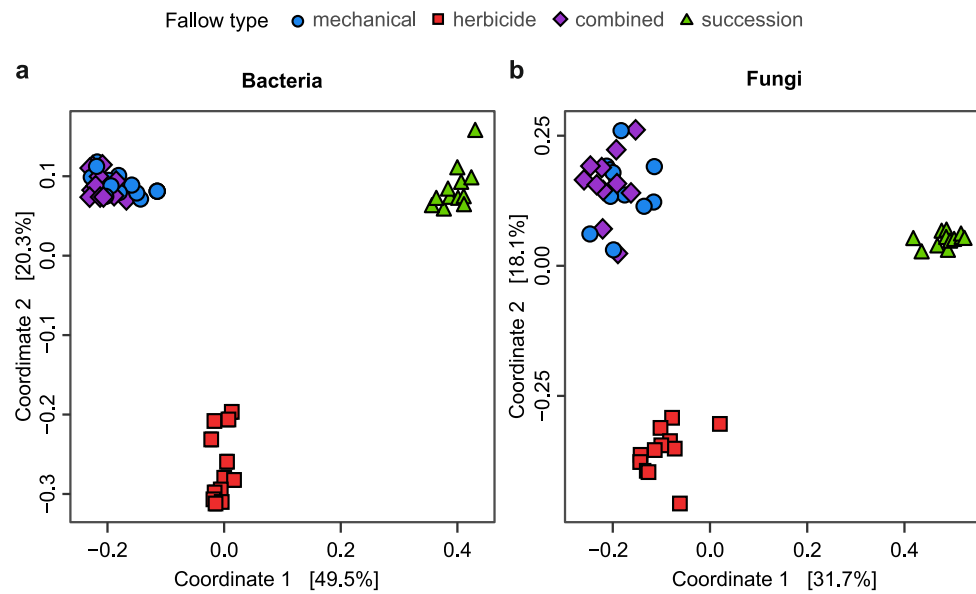


**Fig. 8.** Principal coordinates analysis of (a) bacterial and (b) fungal communities. PERMANOVA results and pairwise comparisons are summarized in Table S4.

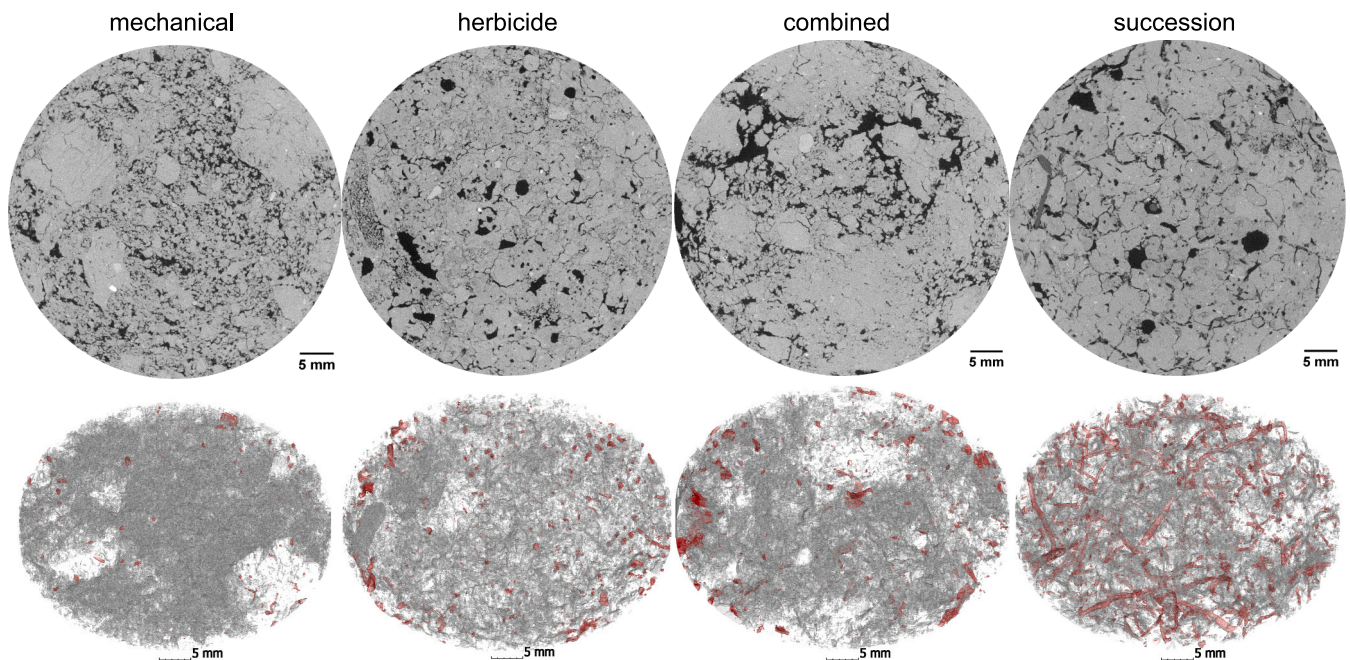


**Fig. 9.** Representative horizontal sections of typical microstructure in intact soil cores displayed as two-dimensional gray-scale information of the original tomograms (top) and as three-dimensional sections with a vertical dimension of 5 mm, centered around the two-dimensional slice displaying macroporosity in transparent gray and particulate organic matter in transparent red (bottom). (For interpretation of the references to colour in this figure legend, the reader is referred to the web version of this article.)

empty root channels were singled out from the composite bioporosity class, these two treatments were identical and only the destruction by tillage remained (Fig. 10d). Mean macropore diameter resembled bioporosity results with a 2.5-fold increase from tilled fallows to natural succession and the herbicide fallow ranging in between (Fig. 10e). The volumetric POM content was 6.4-fold increased in the natural succession compared to bare fallows, which did not differ from each other (Fig. 6f).

### 3.5. Hydraulic properties

The field water content at sampling (Fig. 11a) was highest in the natural succession and was in the range of field capacity (pF 1.8–2.5).

The water content in all bare fallows corresponded to a matric potential of pF 3 (–1000 hPa) or drier. Water retention curves across the entire matric potential range are shown in Fig. S10a. The water contents at selected matric potentials in the wet range (Fig. 11b–c) indicated that the water retention was highest in the natural succession at low suctions, but the differences disappeared when approaching field capacity.

Unsaturated hydraulic conductivity around field capacity (pF 2) was about 4 times higher in the herbicide fallow compared to the tilled fallows. This difference vanished when drained to pF 3. Unsaturated hydraulic conductivity was lowest in the natural succession at both matric potentials (Fig. 11d–e).

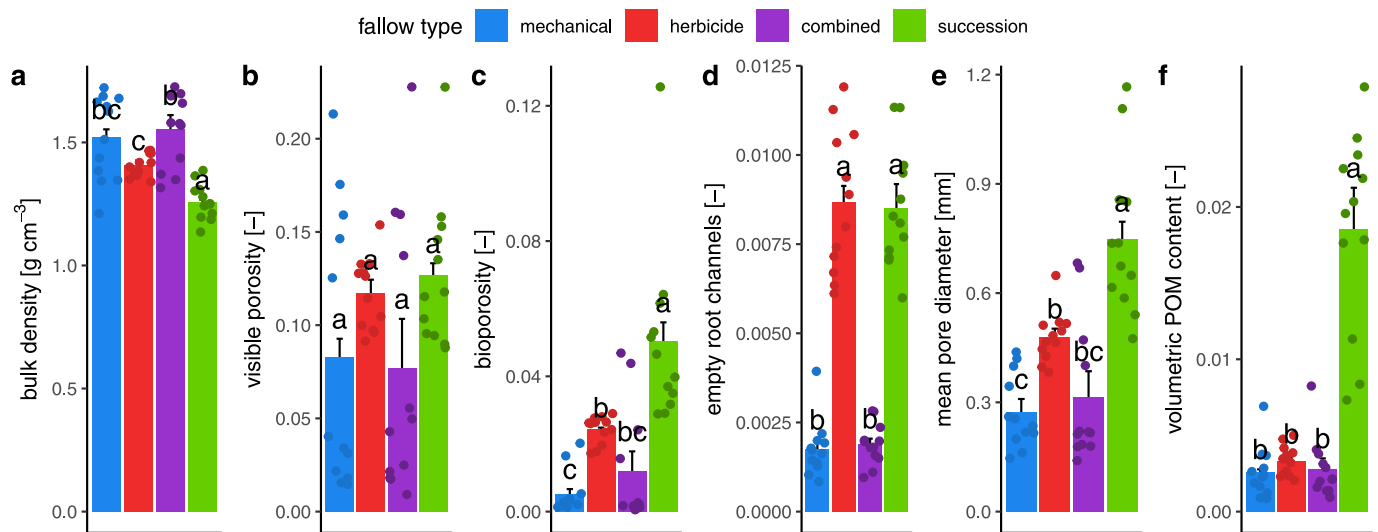


**Fig. 10.** Bulk density (a) and selected microstructural features (b-f) of the fallow treatment (mean  $\pm$  standard error,  $n = 4$ ). Jitter points correspond to individual soil cores ( $n = 16$ ). Significant differences in treatment means at the plot level were tested at  $p = 0.05$ .

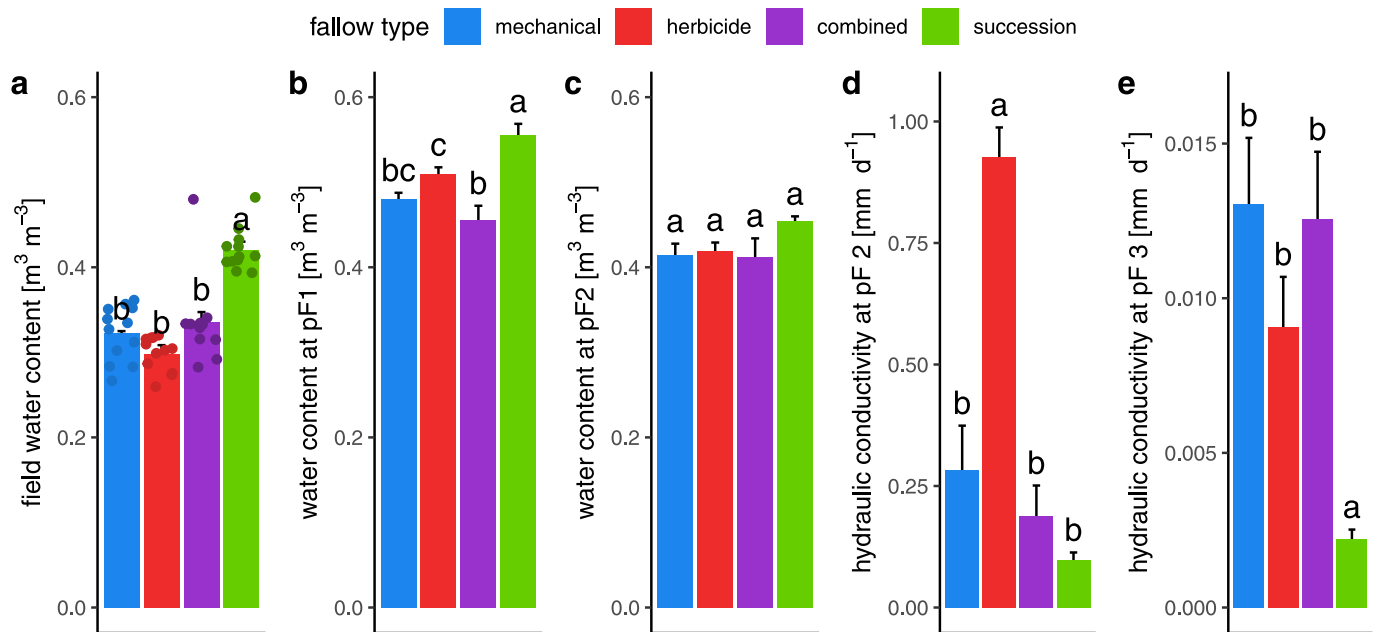


**Fig. 11.** Field water content (a) and hydraulic properties at selected matric potentials (b-e) of the fallow treatments (mean  $\pm$  standard error,  $n = 4$ ). Jitter points in (a) correspond to individual soil cores ( $n = 16$ ). Significant differences in treatment means were tested at  $p = 0.05$ .

### 3.6. Relationship between biological activity and microstructure

Basal respiration was the only biochemical property measured at the soil core level. Therefore, this integrative metric of biological activity lent itself to correlation analysis with microstructure metrics. The strongest association was observed for POM volume fraction ( $R = 0.87$ ), which did not only reflect the differences in basal respiration between natural succession and bare fallows but also the variation with individual cores under natural succession. The two samples with elevated basal respiration under herbicide fallow contained a brood cell with bee eggs or an earthworm (Fig. 12, insets, 2D sections in Fig. S11). Less strong associations with basal respiration were observed for water content ( $R = 0.66$ , Fig. 12b) and bulk density ( $R = -0.64$ , Fig. 12c), which were mainly driven by the difference between natural succession and bare fallows.

Feeding activity was compared with physical and chemical soil

properties at the plot level. Feeding activity had weaker associations with POM content ( $P = 0.68$ , Fig. 12d), than water content ( $R = 0.86$ , Fig. 12e), and also reflected the variation with treatments less well. Interestingly, feeding activity was not correlated at all with mesofauna abundance (Fig. 12f) even though both are elevated under natural succession. A positive correlation would still be weak ( $p = 0.19$ ) if one herbicide plot with exceptionally high mesofauna abundance was excluded from the regression analysis.

## 4. Discussion

### 4.1. Long-term effects of diverging biomass input on soil organic carbon

The first hypothesis that a dynamic equilibrium in total organic carbon would be reached faster in the bare fallows than in the natural succession was confirmed by the data. The rapid decline in TOC contents

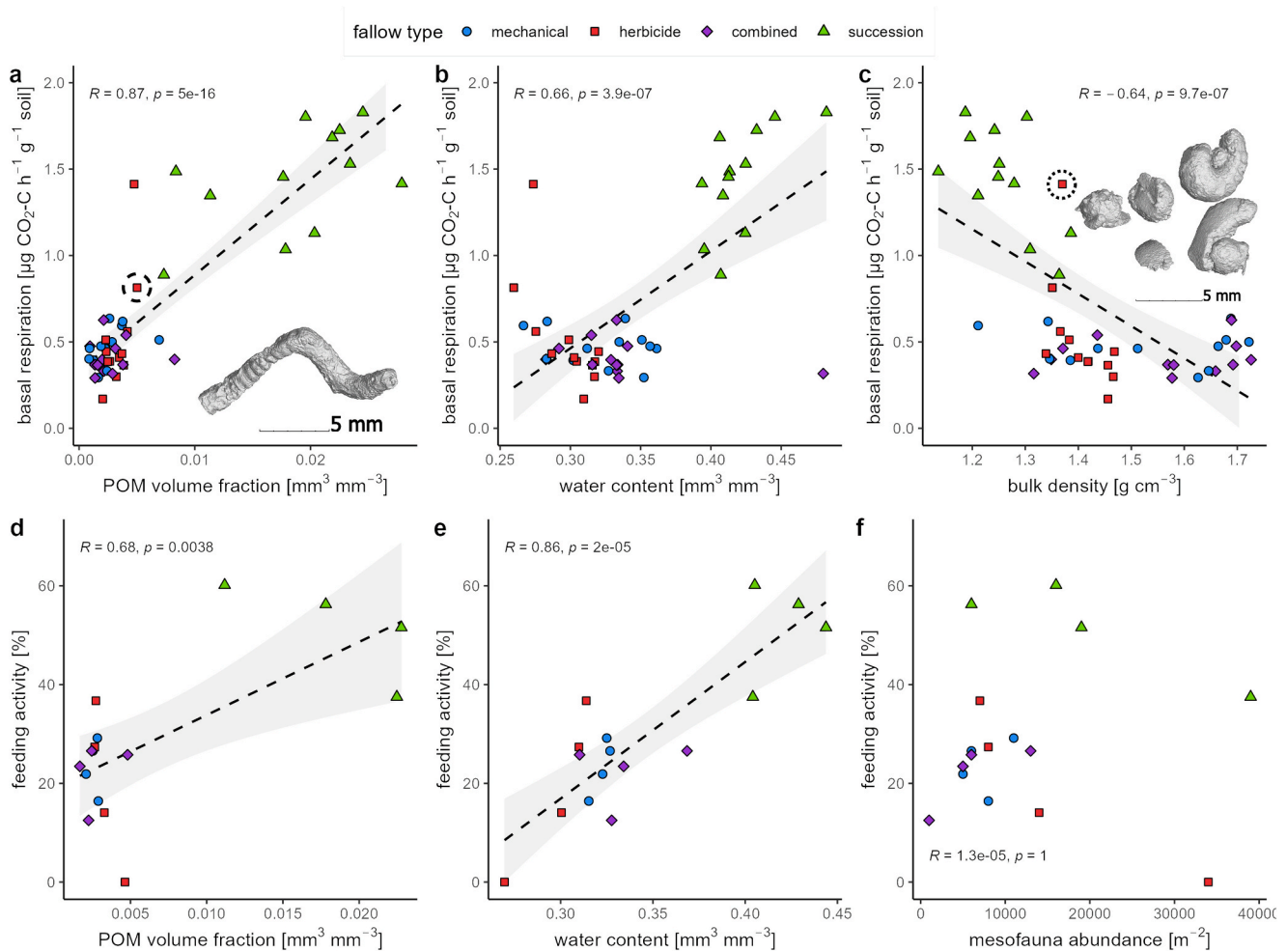


**Fig. 12.** Associations of basal respiration with selected physical properties (a-c) at the soil core level and associations of feeding activity with selected physical properties and mesofauna abundance (d-f) at the plot level. The 3D renderings in (a) and (c) depict an earthworm and a bee nest that was contained in the sample indicated by the dashed and dotted circle, respectively.

during the first ten years of bare fallow matches the early dynamics of many other long-term bare fallow trials (Barré et al., 2010; Meyer et al., 2017). The relative decline at both soil depths only amounted to 20 %, since long-term cropland as the previous land use had already strained carbon stocks before. A rather stable plateau at  $14 \text{ mg C g}^{-1}$  was reached already after 10 years in the subsoil, whereas the topsoil carbon contents of all three bare fallows were at  $16 \text{ mg C g}^{-1}$  and might continue to decline at very low rates in the future as indicated by late-stage dynamics of other long-term bare fallow trials (Barré et al., 2010). The topsoil carbon content of a nearby microplot experiment has a bare soil treatment that was kept bare by hoeing and manual weeding since 1956. This topsoil also approached  $14 \text{ mg C g}^{-1}$  (Schulz, 2002), which might reflect a long-term equilibrium value for this Chernozem soil. The reduction of organic input led to a steady decline in N contents even after the C contents had been stabilized. Labile organic matter fractions associated with plant inputs as observed in the succession samples had vanished in all bare fallow treatments, resulting in a reduction of low-molecular weight saturated and oxidized compounds containing also N and S. Low energy (C-H depleted) as well as aromatic (C-O depleted) and condensed formulas that are indicative of pyrogenic carbon (Barré et al., 2016) were relatively more abundant in the bare fallow treatments. High black carbon contents of  $3 \text{ mg g}^{-1}$  with a relative contribution to organic C of 13 % and a large share of fossil C with high radiocarbon ages (coal, coke and soot particles) have been reported for the site (Brodowski et al., 2007), which are most likely the origin of small compact POM particles (Brodowski et al., 2005; Schlüter et al.,

2022) detected with X-ray CT. However, in the absence of other C inputs, the high share of (condensed) aromatic formulas might also reflect the preferential ionization of aromatic compounds with laser desorption/ionization. The relative accumulation of N-rich microbial biomass as observed in other long-term bare fallow trials (Barré et al., 2018) was also observed here, but was less dominant than the relative accumulation of (condensed) aromatic C. Diverging trends in the oxidation index of long-term persistent organic matter across various long-term bare fallow experiments had been ascribed to different pyrogenic carbon contents before (Barré et al., 2016). Yet, such a high pyrogenic carbon content is likely a specific feature of this site, compared to other long-term bare fallow experiments. The increasing relative contribution of pyrogenic C to TOC might have caused the gradual increase in C:N ratios in the topsoil that only started after twenty years of continuous bare soil management. Likewise, the relative accumulation of carbon of different origins and long-term persistence might also have caused the two-stage behavior of C:N dynamics in the subsoil with a transition after 10–15 years. Initially, the relative decline of plant-derived carbon compared to microbial-derived carbon decreased the C:N ratio. Eventually, the relative contribution of plant and microbial-derived carbon declined compared to the long-term persistent pyrogenic carbon causing the C:N ratio to increase again. The fraction of organic matter that had accumulated in the succession plots was much less condensed, and can be related to plant inputs by experimental design, which was also reflected by a higher POM volume fraction. The plant-derived inputs also drove the accumulation of N and S via microbial recycling (Roth et al., 2019).

One should however note that this accumulation likely is overestimated here due to the comparison to bare fallow soils after 36 years of organic matter decline. A more exact estimate could be derived from a comparison with samples from the start of the experiment.

The increase in TOC contents after conversion of cropland to natural succession was driven by organic inputs of plant-derived origin, reaching  $30 \text{ mg g}^{-1}$  after 36 years, and is bound to steadily increase further. The addition of very high organic fertilizer amounts of up to  $18.7 \text{ Mg C ha}^{-1} \text{ yr}^{-1}$  plowed into the soil in the adjacent 40-year old long-term farmyard manure increase experiment (v494 experiment) raised the TOC content to  $36 \text{ mg g}^{-1}$  under long-term bare fallow (Heinemann et al., 2024). The TOC content was elevated to  $56 \text{ mg g}^{-1}$  under crop rotation with an additional  $1.5 \text{ Mg C ha}^{-1} \text{ yr}^{-1}$  of aboveground organic residues and an unknown amount of belowground C input in the same experiment. The average aboveground net primary production of natural succession is unknown, but estimated to be in the range of an adjacent extensive meadow amounting to  $2.5 \text{ Mg C ha}^{-1} \text{ yr}^{-1}$  (Korell et al., 2024) and is perhaps 4–5 times as high if the total net primary production including root growth is considered (Amos & Walters, 2006; Mokany et al., 2006; Poeplau, 2016). It is conceivable that the long-term natural succession has a dynamic equilibrium TOC content in the range of  $36\text{--}56 \text{ mg g}^{-1}$  at this site, as the lack of soil disturbance may partially compensate for the lower C input. A meta-study on land-use changes under temperate climate indicated that it may take more than 120 years to reach this dynamic equilibrium (Poeplau et al., 2011).

The divergence of organic carbon contents due to the absence or presence of organic inputs caused an even stronger divergence in labile carbon pools and enzyme activity which supports the hypothesized strong impact of plants on soil biochemistry. The normalized respiration rate (per g C) was similar under natural succession and bare fallows, indicating that the higher water content under natural succession had a small effect on basal respiration. The vegetation cover had reduced soil evaporation losses, whereas plant transpiration losses were still low early in the growing season. This order of water contents between natural succession and bare fallows is bound to change towards summer when transpiration losses exceed evaporation losses at this soil depth.

In line with the fourth hypothesis, the long-term absence of organic inputs in the bare fallows caused strong community shifts for fungi and bacteria, which also reduced fungal, but not bacterial alpha diversity. While the dominant bacterial phyla were relatively stable, certain taxa exhibited fallow type-specific shifts. The increased abundance of Proteobacteria under natural succession suggests that steady organic inputs support copiotrophic bacteria, which thrive in substrate and nutrient-rich environments (Fierer et al., 2007; Fierer et al., 2011). Conversely, the reduction of Firmicutes under natural succession may indicate a decline in spore-forming bacteria that are more adapted to disturbed and stressed soils (Xie et al., 2021; Xu et al., 2018). The ordination analysis based on community dissimilarity further confirms the clear separation of the microbial communities in the natural succession fallow from the three bare fallows. This is caused by the very low C input into these systems which limits microbial growth and community diversity. The natural succession, by contrast, fosters a unique microbial assemblage, due to long-term stabilization of soil conditions and high plant diversity (Prommer et al., 2020).

#### 4.2. Contrasting long-term effects between herbicide and mechanical bare fallows

Plowing of the mechanical and combined fallow did not result in a faster and steeper decline in carbon contents of topsoils as compared to the herbicide fallow. The average carbon content under herbicide fallow was consistently higher at all times in both soil depths, but the differences were minimal and only exceeded spatial variation in the subsoil. The soil surface of plowed plots was a few cm deeper than herbicide bare fallow and natural succession plots (Fig. S12) perhaps due to soil compaction and lateral soil transport by machinery. The shifted

reference height might have contributed to lower TOC contents in the subsoil and stresses the need to estimate carbon stocks on an equivalent soil mass basis in the future. An earlier comparison of TOC contents in the topsoil indicated a trend towards a stronger decline under mechanical fallow (Franko & Merbach, 2017) that has now vanished again. This is in line with findings from a long-term experiment conducting a two-year crop rotation with wheat and bare fallow under similar climatic conditions, soil texture, and initial conditions that observed no significant difference in topsoil carbon stocks (0–30 cm) between herbicide and mechanical fallow after 11 years and 27 years, despite consistently higher C stocks under herbicide fallow (Doran et al., 1998). The second hypothesis was therefore falsified by the data, indicating that compromising physical protection of soil carbon by tillage is less relevant than the absence of organic inputs for the decline in total organic carbon. This confirms earlier findings that the effect of physical disturbance on C mineralization rates is negligible compared to the paramount role of C inputs (Mary et al., 2020). Notably, we observed a subtle but significant differentiation of herbicide from mechanical treatments in the molecular composition of soil organic matter. Molecules associated to herbicide fallow were of lower molecular weight, less aromatic, more reduced and enriched in S. The S-bearing herbicide Prosulfocarb was applied on the plots in 2007–2014 at a rate that corresponds to a total amount of  $10.3 \text{ kg ha}^{-1}$  or  $43 \text{ g per plot}$  (Table S1). In contrast, the few compounds associated to mechanical fallow were dominantly N-containing condensed aromatics (CHN, CHNO class). These trends indicate that herbicide application favored the accumulation of a fraction of presumably labile S-containing compounds at the expense of stable N-containing, but the cause of this divergence remains unclear and the overall effect on the molecular composition of SOM (as measured by LDI-FT-ICR-MS) remained small.

Moreover, herbicide and mechanical fallow differed fundamentally in the composition of their soil microbiomes. Fungal phyla were more sensitive to fallow management than bacterial taxa, in particular in response to soil tillage. As expected, Ascomycota remained the dominant fungal phylum across all treatments (Egidi et al., 2019), but their relative abundance varied substantially. The lowest Ascomycota and Basidiomycota representation in the plowed bare fallows (mechanical and combined) suggests that in addition to C-poor environments (Grinhut et al., 2007; Manici et al., 2024) soil disturbance may particularly reduce the abundance of these phyla, contrary to a previous study (Schmidt et al., 2019). In contrast, Chytridiomycota and Mortierellomycota were more prevalent in the plowed fallows, potentially reflecting that they are weak competitors (Freeman et al., 2009), benefiting from the loss of Ascomycota and Basidiomycota species. Such favorable conditions for weak competitors might have also increased fungal richness in the tilled bare fallows compared to the herbicide fallow. The high similarity between mechanical and combined fallows, along with the clear separation from the herbicide fallow, indicates that soil tillage steers bacterial and fungal communities. This is likely caused by the mechanical destruction of fungal hyphae, the disruption of microbial networks, and the reordering of microhabitats (Young & Ritz, 2000). Our findings indicate that long-term herbicide application itself either has no impact on the microbial community or that the impact is negligible compared to that of soil tillage or the absence of plants.

#### 4.3. Divergence in physical, chemical, and biological soil properties

The design of the long-term trial facilitated the combined assessment of the long-term absence or presence of soil tillage and root growth, its effect on soil structure development, and other soil properties that are affected by it. Our third hypothesis that the herbicide fallow would have conserved the typical soil structure of a plow horizon from the beginning of the experiment and therefore be similar to the recent plow horizon in the mechanical bare fallow was falsified by the data. The cessation of plowing caused the formation of a consolidated soil matrix that was pervaded by biopores.

The plowed fallows differed from the herbicide fallow in many ways. The bulk density was on average higher and had greater variability. Soil cores containing large compact clods featured bulk densities  $> 1.6 \text{ g cm}^{-3}$  and macroporosities  $< 0.05 \text{ mm}^3 \text{ mm}^{-3}$  indicative of soil compaction (Kaufmann et al., 2010). When soil cores featured loose, unconsolidated soil in between soil clods, six months after plowing it had already collapsed to a bulk density comparable to no-till soil. The increase in average bulk density with decreasing TOC content may indicate a loss in structural stability against compaction by mechanical stresses by this important binding agent in periodically disturbed soil (Or et al., 2021).

The bioporosity and especially the volume density of empty root channels was elevated in the herbicide fallow to values in the same range as the natural succession even though the POM volume density was negligible and in the same range as the plowed bare fallows. Weed emergence can never be fully suppressed in bare fallows and even very sparse vegetation can accumulate a dense network of root channels over decades, when the soil structure never gets disturbed. The higher abundance of root residues in the shallow topsoil of the herbicide fallows compared to both plowed fallows indicated that weed emergence perhaps from the previous growing season facilitated such biopore formation. Visual inspection in spring indicated the presence of ground-nesting bees in the herbicide fallows perhaps due to the favorable thermal and morphological properties of its soil surface. These soil engineers form their own habitats which resemble anecic earthworm burrows in terms of morphology and pore diameter and also contribute to bioporosity (Tschanz et al., 2023).

The effect of different microstructure on water retention at pF 2 was negligible, but the effect on hydraulic conductivity at pF 2 was strong. This is because the volume fraction of air-filled pores at this matric potential was approximately the same, but the degree to which they block water flow by their spatial configuration was quite different. The fragmented soil matrix in plowed soil imposes a capillary barrier for evaporative flux by the smaller cross-section and higher tortuosity of water flow through contact areas of soil clods (Carminati et al., 2008; Willis & Bond, 1971). Surprisingly, the natural succession featured the lowest unsaturated hydraulic conductivity across all matric potentials despite the absence of plowing. The microstructure was pervaded by curvy, planar pores that seemed to follow old biopore walls and boundaries of earthworm casts in this bioturbated soil. Though small in aperture they form a network of capillary barriers that massively reduce evaporative flux. This could be another reason for the higher field water content under natural succession at the sampling time in spring. These microcracks seemed to be less abundant in the herbicide fallow so that they did not act as capillary barriers at pF 2 causing the highest unsaturated conductivity of all treatments.

The bare fallows and natural succession also diverged in terms of nutrient cycling. None of the treatments had been fertilized and the P input through herbicides such as glyphosate (applied since 2003 in the herbicide and combined bare fallow, Table S1) was negligible compared to available P at the beginning of the long-term experiment. Yet, the available K content in the shallow topsoil was elevated under natural succession with effect sizes similar to water-extractable carbon and nitrogen, whereas available P did not differ at all. As a consequence, the increase in phosphatase activity from bare fallows to natural succession indicative of P cycling was much smaller (3.4-fold), than the increase in  $\beta$ -glucosidase (12.4 fold) and N-acetylglucosaminidase activity (13-fold) indicative of C and N cycling, respectively. In the long-term, the climatic water balance was sufficient to induce a net downward transport of the moderately mobile  $\text{K}^+$  cations, which were therefore leached from the shallow topsoil under bare fallow, but pumped back and recycled through root uptake and decay under natural succession (Chadwick & Chorover, 2001; Porder & Chadwick, 2009). Such vertical redistribution and cycling were less relevant for the strongly sorbed  $\text{PO}_4^{3-}$  anions.

## 5. Conclusions

The long-term bare fallow experiment V505a in Bad Lauchstädt provides a rare opportunity to study the effects of soil tillage, herbicide application, and organic inputs by plant growth in isolation. We showed that all factors have far-reaching and very different consequences for a range of chemical, biological, and hydraulic soil properties.

Plant effects on soil ecosystems go beyond the maintenance of higher microbial and faunal activity by input of organic carbon. They foster a range of processes like nutrient uplift, soil structure formation by root growth, carbon-mediated structure stability, and protection against bare soil evaporation by plant cover. The long-term absence of plants at this site caused a relative enrichment of presumably long-term stable pyrogenic carbon and to a lesser degree of compounds derived from microbial biomass. The decreasing carbon content in the absence of plant input was not markedly intensified by tillage. Soil tillage periodically destroyed bioporosity and reduced unsaturated hydraulic conductivity by soil loosening. It affected fungi more than bacteria and the microbial community more than the quantity and quality of organic matter. The impact of tillage on microbial communities was much stronger than the impact of herbicides.

This study provides an excellent test case for holistic ecosystem modeling that captures several soil functions at the relevant temporal and spatial scales like carbon and nutrient cycling, soil hydraulic properties, and the maintenance of soil biodiversity.

### CRedit authorship contribution statement

**Steffen Schlüter:** Writing – original draft, Visualization, Validation, Investigation, Formal analysis, Data curation, Conceptualization. **Mengqi Wu:** Writing – review & editing, Formal analysis, Data curation. **Maxime Phalempin:** Writing – review & editing, Software. **Lena Philipp:** Writing – review & editing, Visualization, Formal analysis, Data curation. **Evgenia Blagodatskaya:** Writing – review & editing, Formal analysis. **Thomas Reitz:** Writing – review & editing, Writing – original draft, Validation, Formal analysis, Data curation. **Carsten Simon:** Writing – original draft, Visualization, Validation, Formal analysis, Data curation. **Oliver Lechtenfeld:** Writing – review & editing. **Hans-Jörg Vogel:** Writing – review & editing. **Martin Schädler:** Writing – review & editing, Supervision, Data curation. **Ines Merbach:** Writing – review & editing, Validation, Supervision, Project administration, Investigation, Formal analysis, Data curation.

### Declaration of competing interest

The authors declare that they have no known competing financial interests or personal relationships that could have appeared to influence the work reported in this paper.

### Acknowledgments

We thank the students of the master module “Soil Structure Analysis” at the Martin-Luther University Halle Wittenberg for sampling and laboratory analysis and Shang Wang for providing microbial biomass data.

The scientific results have (in part) been computed at the High-Performance Computing (HPC) Cluster EVE, a joint effort of both the Helmholtz Centre for Environmental Research (<http://www.ufz.de/>) and the German Centre for Integrative Biodiversity Research Halle-Jena Leipzig (<http://www.idiv-biodiversity.de/>). We would like to thank the administration and support staff of EVE who keep the system running and support us with our scientific computing needs: Thomas Schnicke, Ben Langenberg, Guido Schramm, Toni Harzendorf, Tom Stempel and Lisa. Schurack from the UFZ, and Christian Krause from iDiv.

## Appendix A. Supplementary data

Supplementary data to this article can be found online at <https://doi.org/10.1016/j.geoderma.2025.117361>.

## Data availability

All processed data is accessible at doi:10.48758/ufz.15787. Sequencing data is available at the Sequencing Read Archive (SRA) through the accession number PRJNA1240206.

## References

- Amos, B., Walters, D.T., 2006. Maize root biomass and net rhizodeposited carbon. *Soil Sci. Soc. Am. J.* 70 (5), 1489–1503. <https://doi.org/10.2136/sssaj2005.0216>.
- Bacq-Labreuil, A., Crawford, J., Mooney, S.J., Neal, A.L., Akkari, E., McAuliffe, C., Zhang, X., Redmile-Gordon, M., Ritz, K., 2018. Effects of cropping systems upon the three-dimensional architecture of soil systems are modulated by texture. *Geoderma* 332, 73–83. <https://doi.org/10.1016/j.geoderma.2018.07.002>.
- Balabane, M., Plante, A.F., 2004. Aggregation and carbon storage in silty soil using physical fractionation techniques. *Eur. J. Soil Sci.* 55 (2), 415–427. <https://doi.org/10.1111/j.1351-0754.2004.0608.x>.
- Barré, P., Eglin, T., Christensen, B.T., Ciais, P., Houot, S., Kätterer, T., van Oort, F., Peylin, P., Poulton, P.R., Romanenkov, V., Chenu, C., 2010. Quantifying and isolating stable soil organic carbon using long-term bare fallow experiments. *Biogeosciences* 7 (11), 3839–3850. <https://doi.org/10.5194/bg-7-3839-2010>.
- Barré, P., Plante, A.F., Cécillon, L., Lutfalla, S., Baudin, F., Bernard, S., Christensen, B.T., Eglin, T., Fernandez, J.M., Houot, S., Kätterer, T., Le Guillou, C., Macdonald, A., van Oort, F., Chenu, C., 2016. The energetic and chemical signatures of persistent soil organic matter. *Biogeochemistry* 130 (1), 1–12. <https://doi.org/10.1007/s10533-016-0246-0>.
- Barré, P., Quénéa, K., Vidal, A., Cécillon, L., Christensen, B.T., Kätterer, T., Macdonald, A., Petit, L., Plante, A.F., van Oort, F., Chenu, C., 2018. Microbial and plant-derived compounds both contribute to persistent soil organic carbon in temperate soils. *Biogeochemistry* 140 (1), 81–92. <https://doi.org/10.1007/s10533-018-0475-5>.
- Bates, D., Mächler, M., Bolker, B., Walker, S., 2015. Fitting linear mixed-effects models using lme4. *J. Stat. Softw.* 67 (1), 1–48. <https://doi.org/10.18637/jss.v067.i01>.
- Brodowski, S., Amelung, W., Haumaier, L., Abetz, C., Zech, W., 2005. Morphological and chemical properties of black carbon in physical soil fractions as revealed by scanning electron microscopy and energy-dispersive X-ray spectroscopy. *Geoderma* 128 (1), 116–129. <https://doi.org/10.1016/j.geoderma.2004.12.019>.
- Brodowski, S., Amelung, W., Haumaier, L., Zech, W., 2007. Black carbon contribution to stable humus in German arable soils. *Geoderma* 139 (1), 220–228. <https://doi.org/10.1016/j.geoderma.2007.02.004>.
- Carminati, A., Kaestner, A., Lehmann, P., Flühtler, H., 2008. Unsaturated water flow across soil aggregate contacts. *Adv. Water Resour.* 31 (9), 1221–1232. <https://doi.org/10.1016/j.advwatres.2008.01.008>.
- Chadwick, O.A., Chorover, J., 2001. The chemistry of pedogenic thresholds. *Geoderma* 100, 321–353.
- Conant, R.T., Easter, M., Paustian, K., Swan, A., Williams, S., 2007. Impacts of periodic tillage on soil C stocks: A synthesis. *Soil Tillage Res.* 95 (1), 1–10. <https://doi.org/10.1016/j.still.2006.12.006>.
- DIN ISO 13878, 1998. Bodenbeschaffenheit-Bestimmung des Gesamt-Stickstoffs durch trockene Verbrennung (Elementaranalyse). Beuth-Verlag, Berlin.
- Doran, J.W., Elliott, E.T., Paustian, K., 1998. Soil microbial activity, nitrogen cycling, and long-term changes in organic carbon pools as related to fallow tillage management. *Soil Tillage Res.* 49 (1), 3–18. [https://doi.org/10.1016/S0167-1987\(98\)00150-0](https://doi.org/10.1016/S0167-1987(98)00150-0).
- Dungait, J.A.J., Hopkins, D.W., Gregory, A.S., Whitmore, A.P., 2012. Soil organic matter turnover is governed by accessibility not recalcitrance. *Glob. Chang. Biol.* 18 (6), 1781–1796. <https://doi.org/10.1111/j.1365-2486.2012.02665.x>.
- Egidi, E., Delgado-Baquerizo, M., Plett, J.M., Wang, J., Eldridge, D.J., Bardgett, R.D., Maestre, F.T., Singh, B.K., 2019. A few Ascomycota taxa dominate soil fungal communities worldwide. *Nat. Commun.* 10 (1), 2369. <https://doi.org/10.1038/s41467-019-10373-z>.
- Fierer, N., Bradford, M.A., Jackson, R.B., 2007. Toward an ecological classification of soil bacteria. *Ecology* 88 (6), 1354–1364. <https://doi.org/10.1890/05-1839>.
- Fierer, N., Lauber, C.L., Ramirez, K.S., Zaneveld, J., Bradford, M.A., Knight, R., 2011. Comparative metagenomic, phylogenetic and physiological analyses of soil microbial communities across nitrogen gradients. *ISME J.* 6 (5), 1007–1017. <https://doi.org/10.1038/ismej.2011.159>.
- Fox, J., & Weisberg, S. (2011). An R Companion to Applied Regression. <http://socserv.socsci.mcmaster.ca/jfox/Books/Companion>.
- Franko, U., Merbach, I., 2017. Modelling soil organic matter dynamics on a bare fallow Chernozem soil in Central Germany. *Geoderma* 303, 93–98. <https://doi.org/10.1016/j.geoderma.2017.05.013>.
- Freeman, K.R., Martin, A.P., Karki, D., Lynch, R.C., Mitter, M.S., Meyer, A.F., Longcore, J.E., Simmons, D.R., Schmidt, S.K., 2009. Evidence that chytrids dominate fungal communities in high-elevation soils. *Proc. Natl. Acad. Sci.* 106 (43), 18315–18320. <https://doi.org/10.1073/pnas.0907303106>.
- George, P.B.L., Fidler, D.B., Van Nostrand, J.D., Atkinson, J.A., Mooney, S.J., Creer, S., Griffiths, R.I., McDonald, J.E., Robinson, D.A., Jones, D.L., 2021. Shifts in soil structure, biological, and functional diversity under long-term carbon deprivation. *Front. Microbiol.* 12. <https://doi.org/10.3389/fmicb.2021.735022>.
- Grinhut, T., Hadar, Y., Chen, Y., 2007. Degradation and transformation of humic substances by saprotrophic fungi: processes and mechanisms. *Fungal Biol. Rev.* 21 (4), 179–189. <https://doi.org/10.1016/j.fbr.2007.09.003>.
- Guo, L.B., Gifford, R.M., 2002. Soil carbon stocks and land use change: a meta analysis. *Glob. Chang. Biol.* 8 (4), 345–360. <https://doi.org/10.1046/j.1354-1013.2002.00486.x>.
- Haghighi, E., Or, D., 2015. Evaporation from wavy porous surfaces into turbulent airflows. *Transp. Porous Media* 110 (2), 225–250. <https://doi.org/10.1007/s11242-015-0512-y>.
- Hawkes, J.A., D'Andrilli, J., Agar, J.N., Barrow, M.P., Berg, S.M., Catalán, N., Chen, H., Chu, R.K., Cole, R.B., Dittmar, T., Gavard, R., Gleixner, G., Hatcher, P.G., He, C., Hess, N.J., Hutchins, R.H.S., Ijaz, A., Jones, H.E., Kew, W., Podgorski, D.C., 2020. An international laboratory comparison of dissolved organic matter composition by high resolution mass spectrometry: Are we getting the same answer? *Limnol. Oceanogr. Methods* 18 (6), 235–258. <https://doi.org/10.1002/lom3.10364>.
- Heinemann, H., Don, A., Poeplau, C., Merbach, I., Reinsch, T., Welp, G., Vos, C., 2024. No saturation of soil carbon under long-term extreme manure additions. *Plant Soil*. <https://doi.org/10.1007/s11104-024-07146-z>.
- Hirsch, P.R., Gilliam, L.M., Sohi, S.P., Williams, J.K., Clark, I.M., Murray, P.J., 2009. Starving the soil of plant inputs for 50 years reduces abundance but not diversity of soil bacterial communities. *Soil Biol. Biochem.* 41 (9), 2021–2024. <https://doi.org/10.1016/j.soilbio.2009.07.011>.
- Hirsch, P.R., Jhurrea, D., Williams, J.K., Murray, P.J., Scott, T., Misselbrook, T.H., Goulding, K.W.T., Clark, I.M., 2017. Soil resilience and recovery: rapid community responses to management changes. *Plant Soil* 412 (1), 283–297. <https://doi.org/10.1007/s11104-016-3068-x>.
- Isensee, F., Jaeger, P.F., Kohl, S.A.A., Petersen, J., Maier-Hein, K.H., 2021. nnU-Net: a self-configuring method for deep learning-based biomedical image segmentation. *Nat. Methods* 18 (2), 203–211. <https://doi.org/10.1038/s41592-020-01008-z>.
- Joergensen, R.G., Hemkemeyer, M., Beule, L., Iskakova, J., Oskonbaeva, Z., Rummel, P. S., Schwalb, S.A., Wichern, F., 2024. A hitchhiker's guide: estimates of microbial biomass and microbial gene abundance in soil. *Biol. Fertil. Soils* 60 (4), 457–470. <https://doi.org/10.1007/s00374-024-01810-3>.
- Kallenbach, C.M., Frey, S.D., Grandy, A.S., 2016. Direct evidence for microbial-derived soil organic matter formation and its ecophysiological controls. *Nat. Commun.* 7 (1), 13630. <https://doi.org/10.1038/ncomms13630>.
- Kaufmann, M., Tobias, S., Schulin, R., 2010. Comparison of critical limits for crop plant growth based on different indicators for the state of soil compaction. *J. Plant Nutr. Soil Sci.* 173 (4), 573–583. <https://doi.org/10.1002/jpln.200900129>.
- Kim, S., Kramer, R.W., Hatcher, P.G., 2003. Graphical method for analysis of ultrahigh-resolution broadband mass spectra of natural organic matter, the Van Krevelen diagram. *Anal. Chem.* 75 (20), 5336–5344. <https://doi.org/10.1021/ac034415p>.
- Koch, B.P., Dittmar, T., 2006. From mass to structure: an aromaticity index for high-resolution mass data of natural organic matter. *Rapid Commun. Mass Spectrom.* 20 (5), 926–932. <https://doi.org/10.1002/rcm.2386>.
- Koch, B.P., Dittmar, T., 2016. From mass to structure: an aromaticity index for high-resolution mass data of natural organic matter. *Rapid Commun. Mass Spectrom.* 30 (1), 250. <https://doi.org/10.1002/rcm.7433>.
- Korell, L., Andrzejak, M., Berger, S., Durka, W., Haider, S., Hensen, I., Herion, Y., Höfner, J., Kindermann, L., Klotz, S., Knight, T.M., Linstädter, A., Madaj, A.-M., Merbach, I., Michalski, S., Plos, C., Roscher, C., Schädler, M., Welk, E., Auge, H., 2024. Land use modulates resistance of grasslands against future climate and inter-annual climate variability in a large field experiment. *Glob. Chang. Biol.* 30 (7), e17418. <https://doi.org/10.1111/gcb.17418>.
- Kratz, W., 1998. The bait-lamina test. *Environ. Sci. Pollut. Res.* 5 (2), 94–96. <https://doi.org/10.1007/BF02986394>.
- LaRowe, D.E., Van Cappellen, P., 2011. Degradation of natural organic matter: A thermodynamic analysis. *Geochim. Cosmochim. Acta* 75 (8), 2030–2042. <https://doi.org/10.1016/j.gca.2011.01.020>.
- Lefèvre, R., Barré, P., Moyano, F.E., Christensen, B.T., Bardoux, G., Eglin, T., Girardin, C., Houot, S., Kätterer, T., van Oort, F., Chenu, C., 2014. Higher temperature sensitivity for stable than for labile soil organic carbon – Evidence from incubations of long-term bare fallow soils. *Glob. Chang. Biol.* 20 (2), 633–640. <https://doi.org/10.1111/gcb.12402>.
- Lehmann, J., Kleber, M., 2015. The contentious nature of soil organic matter [Perspective]. *Nature* 528, 60. <https://doi.org/10.1038/nature16069>.
- Lenth, R. (2022). emmeans: Estimated marginal means, aka least-squares means. R package version 1.7.2. In.
- Liang, C., Amelung, W., Lehmann, J., Kästner, M., 2019. Quantitative assessment of microbial necromass contribution to soil organic matter. *Glob. Chang. Biol.* 25 (11), 3578–3590. <https://doi.org/10.1111/gcb.14781>.
- Macfadyen, A., 1961. Improved funnel-type extractors for soil arthropods. *J. Anim. Ecol.* 30 (1), 171–184. <https://doi.org/10.2307/2120>.
- Manici, L.M., Caputo, F., Fornasier, F., Paletto, A., Ceotto, E., De Meo, I., 2024. Ascomycota and Basidiomycota fungal phyla as indicators of land use efficiency for soil organic carbon accrual with woody plantations. *Ecol. Ind.* 160, 111796. <https://doi.org/10.1016/j.ecolind.2024.111796>.
- Mary, B., Clivot, H., Błaszczczyk, N., Labreuche, J., Ferchaud, F., 2020. Soil carbon storage and mineralization rates are affected by carbon inputs rather than physical disturbance: Evidence from a 47-year tillage experiment. *Agr. Ecosyst. Environ.* 299, 106972. <https://doi.org/10.1016/j.agee.2020.106972>.

- McMurdie, P.J., Holmes, S., 2013. phyloseq: An R package for reproducible interactive analysis and graphics of microbiome census data. *PLoS One* 8 (4), e61217. <https://doi.org/10.1371/journal.pone.0061217>.
- Meyer, N., Bornemann, L., Welp, G., Schiedung, H., Herbst, M., Amelung, W., 2017. Carbon saturation drives spatial patterns of soil organic matter losses under long-term bare fallow. *Geoderma* 306, 89–98. <https://doi.org/10.1016/j.geoderma.2017.07.004>.
- Mokany, K., Raison, R.J., Prokushin, A.S., 2006. Critical analysis of root:shoot ratios in terrestrial biomes. *Glob. Chang. Biol.* 12 (1), 84–96. <https://doi.org/10.1111/j.1365-2486.2005.001043.x>.
- Murphy, J., Riley, J.P., 1962. A modified single solution method for the determination of phosphate in natural waters. *Anal. Chim. Acta* 27, 31–36. [https://doi.org/10.1016/S0003-2670\(00\)88444-5](https://doi.org/10.1016/S0003-2670(00)88444-5).
- Neal, A.L., Bacq-Labreuil, A., Zhang, X., Clark, I.M., Coleman, K., Mooney, S.J., Ritz, K., Crawford, J.W., 2020. Soil as an extended composite phenotype of the microbial metagenome. *Sci. Rep.* 10 (1), 10649. <https://doi.org/10.1038/s41598-020-67631-0>.
- Oksanen, J., Simpson, G. L., Blanchet, F. G., Kindt, R., Legendre, P., Minchin, P. R., O'Hara, R. B., Solyoms, P., Stevens, M. H. H., Szoecs, E., Wagner, H., Barbour, M., Bedward, M., Bolker, B., Borcard, D., Borman, T., Carvalho, G., Chirico, M., De Caceres, M., . . . Weedon, J. (2025). *vegan: Community Ecology Package*. <https://vegandevs.github.io/vegan/>.
- Or, D., Keller, T., Schlesinger, W.H., 2021. Natural and managed soil structure: On the fragile scaffolding for soil functioning. *Soil Tillage Res.* 208, 104912. <https://doi.org/10.1016/j.still.2020.104912>.
- Palm, C., Blanco-Canqui, H., DeClerck, F., Gater, L., Grace, P., 2014. Conservation agriculture and ecosystem services: An overview. *Agr. Ecosyst. Environ.* 187, 87–105.
- Peixoto, D.S., Silva, L.D.C.M.d., Melo, L.B.B.d., Azevedo, R.P., Araújo, B.C.L., Carvalho, T. S.d., Moreira, S.G., Curi, N., Silva, B.M., 2020. Occasional tillage in no-tillage systems: A global meta-analysis. *Sci. Total Environ.* 745, 140887. <https://doi.org/10.1016/j.scitotenv.2020.140887>.
- Peters, G.-J. Y., & Gruijters, S. (2023). *ufs: A collection of utilities*. <https://ufs.openscience/>.
- Phalempin, M., Krämer, L., Geers-Lucas, M., Isensee, F., Schlüter, S., 2025. Deep learning segmentation of soil constituents in 3D X-ray CT images. *Geoderma* 458, 117321. <https://doi.org/10.1016/j.geoderma.2025.117321>.
- Poelau, C., 2016. Estimating root: shoot ratio and soil carbon inputs in temperate grasslands with the RothC model. *Plant and Soil* 407 (1), 293–305. <https://doi.org/10.1007/s11104-016-3017-8>.
- Poelau, C., Dechow, R., Begill, N., Don, A., 2024. Towards an ecosystem capacity to stabilise organic carbon in soils. *Glob. Chang. Biol.* 30 (8), e17453. <https://doi.org/10.1111/gcb.17453>.
- Poelau, C., Don, A., Vesterdal, L., Leifeld, J., van Wesemael, B., Schumacher, J., Gensior, A., 2011. Temporal dynamics of soil organic carbon after land-use change in the temperate zone – carbon response functions as a model approach. *Glob. Chang. Biol.* 17 (7), 2415–2427. <https://doi.org/10.1111/j.1365-2486.2011.02408.x>.
- Porder, S., Chadwick, O.A., 2009. Climate and soil-age constraints on nutrient uplift and retention by plants. *Ecology* 90 (3), 623–636. <https://doi.org/10.1890/07-1739.1>.
- Post, W.M., Kwon, K.C., 2000. Soil carbon sequestration and land-use change: processes and potential. *Glob. Chang. Biol.* 6 (3), 317–327. <https://doi.org/10.1046/j.1365-2486.2000.00308.x>.
- Prommer, J., Walker, T.W.N., Wanek, W., Braun, J., Zezula, D., Hu, Y., Hofhansl, F., Richter, A., 2020. Increased microbial growth, biomass, and turnover drive soil organic carbon accumulation at higher plant diversity. *Glob. Chang. Biol.* 26 (2), 669–681. <https://doi.org/10.1111/gcb.14777>.
- R Core Team, 2022. *R: A language and environment for statistical computing*. R Foundation for Statistical Computing. R Foundation for Statistical Computing, Vienna, Austria <https://www.R-project.org/>.
- Riedel, T., Zak, D., Biester, H., Dittmar, T., 2013. Iron traps terrestrially derived dissolved organic matter at redox interfaces. *Proc. Natl. Acad. Sci.* 110 (25), 10101–10105. <https://doi.org/10.1073/pnas.1221487110>.
- Roth, V.-N., Lange, M., Simon, C., Hertkorn, N., Bucher, S., Goodall, T., Griffiths, R.I., Mellado-Vázquez, P.G., Mommer, L., Oram, N.J., Weigelt, A., Dittmar, T., Gleixner, G., 2019. Persistence of dissolved organic matter explained by molecular changes during its passage through soil. *Nat. Geosci.* 12 (9), 755–761. <https://doi.org/10.1038/s41561-019-0417-4>.
- Schindelin, J., Arganda-Carreras, I., Frise, E., Kaynig, V., Longair, M., Pietzsch, T., Preibisch, S., Rueden, C., Saalfeld, S., Schmid, B., Tinevez, J.-Y., White, D.J., Hartenstein, V., Eliceiri, K., Tomancak, P., Cardona, A., 2012. Fiji: an open-source platform for biological-image analysis. *Nat. Methods* 9 (7), 676–682. <https://doi.org/10.1038/nmeth.2019>.
- Schlüter, S., Albrecht, L., Schwärzel, K., Kreiselmeier, J., 2020. Long-term effects of conventional tillage and no-tillage on saturated and near-saturated hydraulic conductivity – Can their prediction be improved by pore metrics obtained with X-ray CT? *Geoderma* 361, 114082. <https://doi.org/10.1016/j.geoderma.2019.114082>.
- Schlüter, S., Leuther, F., Albrecht, L., Hoeschen, C., Kilian, R., Surey, R., Mikutta, R., Kaiser, K., Mueller, C.W., Vogel, H.-J., 2022. Microscale carbon distribution around pores and particulate organic matter varies with soil moisture regime. *Nat. Commun.* 13 (1), 2098. <https://doi.org/10.1038/s41467-022-29605-w>.
- Schlüter, S., Leuther, F., Vogler, S., Vogel, H.-J., 2016. X-ray microtomography analysis of soil structure deformation caused by centrifugation. *Solid Earth* 7 (1), 129–140. <https://doi.org/10.5194/se-7-129-2016>.
- Schmidt, R., Mitchell, J., Scow, K., 2019. Cover cropping and no-till increase diversity and symbiotroph:saprotroph ratios of soil fungal communities. *Soil Biol. Biochem.* 129, 99–109. <https://doi.org/10.1016/j.soilbio.2018.11.010>.
- Schulz, E., 2002. Influence of extreme management on decomposable soil organic matter pool. *Arch. Agron. Soil Sci.* 48 (2), 101–105. <https://doi.org/10.1080/03650340214166>.
- Schweizer, S.A., Aehnel, M., Bucka, F., Totsche, K.U., Kögel-Knabner, I., 2024. Impact of bare fallow management on soil carbon storage and aggregates across a rock fragment gradient. *J. Plant Nutr. Soil Sci.* 187 (1), 118–129. <https://doi.org/10.1002/jpln.202300156>.
- Simon, C., Miltner, A., Mulder, I., Kaiser, K., Lorenz, M., Thiele-Bruhn, S., Lechtenfeld, O., 2025. Long-term effects of manure addition on soil organic matter molecular composition: Carbon transformation as a major driver of energetic potential. *Soil Biol. Biochem.* 109755. <https://doi.org/10.1016/j.soilbio.2025.109755>.
- Sinsabaugh, R.L., Saiya-Cork, K., Long, T., Osgood, M.P., Neher, D.A., Zak, D.R., Norby, R.J., 2003. Soil microbial activity in a Liquidambar plantation unresponsive to CO<sub>2</sub>-driven increases in primary production. *Appl. Soil Ecol.* 24 (3), 263–271. [https://doi.org/10.1016/S0929-1393\(03\)00002-7](https://doi.org/10.1016/S0929-1393(03)00002-7).
- Six, J., Doetterl, S., Laub, M., Müller, C.R., Van de Broek, M., 2024. The six rights of how and when to test for soil C saturation. *SOIL* 10 (1), 275–279. <https://doi.org/10.5194/soil-10-275-2024>.
- Six, J., Elliott, E.T., Paustian, K., 1999. Aggregate and soil organic matter dynamics under conventional and no-tillage systems. *Soil Sci. Soc. Am. J.* 63 (5), 1350–1358. <https://doi.org/10.2136/sssaj1999.6351350x>.
- Solihat, N.N., Acter, T., Kim, D., Plante, A.F., Kim, S., 2019. Analyzing solid-phase natural organic matter using laser desorption/ionization ultrahigh resolution mass spectrometry. *Anal. Chem.* 91 (1), 951–957. <https://doi.org/10.1021/acs.analchem.8b04032>.
- Strudley, M.W., Green, T.R., Ascough, J.C., 2008. Tillage effects on soil hydraulic properties in space and time: State of the science. *Soil Tillage Res.* 99 (1), 4–48.
- Tschanz, P., Koestel, J., Volpe, V., Albrecht, M., Keller, T., 2023. Morphology and temporal evolution of ground-nesting bee burrows created by solitary and social species quantified through X-ray imaging. *Geoderma* 438, 116655. <https://doi.org/10.1016/j.geoderma.2023.116655>.
- Verband Deutscher Landwirtschaftlicher Untersuchungs-und Forschungsanstalten (VDLUFA). (2007). *Handbuch der Landwirtschaftlichen Versuchs-und Untersuchungsmethodik (VDLUFA-Methodenbuch)*. VDLUFA-Verlag.
- Verhulst, N., Govaerts, B., Verachert, E., Castellanos-Navarrete, A., Mezzalama, M., Wall, P., Chocobar, A., Deckers, J., Sayre, K., 2010. Conservation agriculture, improving soil quality for sustainable production systems? *Adv. Soil Sci.* 137–208.
- Wardak, D.L.R., Padia, F.N., de Heer, M.I., Sturrock, C.J., Mooney, S.J., 2022. Zero tillage has important consequences for soil pore architecture and hydraulic transport: A review. *Geoderma* 422, 115927. <https://doi.org/10.1016/j.geoderma.2022.115927>.
- Weißbecker, C., Schnabel, B., Heintz-Buschart, A., 2020. Dadasnake, a Snakemake implementation of DADA2 to process amplicon sequencing data for microbial ecology. *GigaScience* 9 (12). <https://doi.org/10.1093/gigascience/giaa135>.
- Wickham, H. (2016). *ggplot2: Elegant Graphics for Data Analysis*. <https://ggplot2.tidyverse.org>.
- Willis, W.O., Bond, J.J., 1971. Soil water evaporation: reduction by simulated tillage. *Soil Sci. Soc. Am. J.* 35 (4), 526–529. <https://doi.org/10.2136/sssaj1971.03615995003500040016x>.
- Wurz, J., Groß, A., Franze, K., Lechtenfeld, O., 2024. Lambda-miner: enhancing reproducible natural organic matter data processing with a semi-automatic web application. EGU General Assembly Conference Abstracts, Vienna, Austria <https://ui.adsabs.harvard.edu/abs/2024EGUGA.2615782W>.
- Xie, J., Dawwam, G.E., Sehim, A.E., Li, X., Wu, J., Chen, S., Zhang, D., 2021. Drought stress triggers shifts in the root microbial community and alters functional categories in the microbial gene pool [Original Research]. *Front. Microbiol.* 12. <https://doi.org/10.3389/fmicb.2021.744897>.
- Xu, L., Naylor, D., Dong, Z., Simmons, T., Pierroz, G., Hixson, K.K., Kim, Y.-M., Zink, E. M., Engbrecht, K.M., Wang, Y., Gao, C., DeGraaf, S., Madera, M.A., Sievert, J.A., Hollingsworth, J., Birdseye, D., Scheller, H.V., Huttmacher, R., Dahlberg, J., Coleman-Derr, D., 2018. Drought delays development of the sorghum root microbiome and enriches for monoderm bacteria. *Proc. Natl. Acad. Sci.* 115 (18), E4284–E4293. <https://doi.org/10.1073/pnas.1717308115>.
- Young, I.M., Ritz, K., 2000. Tillage, habitat space and function of soil microbes. *Soil Tillage Res.* 53, 201–213. [https://doi.org/10.1016/S0167-1987\(99\)00106-3](https://doi.org/10.1016/S0167-1987(99)00106-3).